7. Some Basic Properties of Matter Waves

7.1 Wave Packets

In the two preceding chapters it was shown that light, electrons and other elementary particles can have both wave and particle characteristics. In this chapter we will examine more closely how the wave properties of matter can be understood and described mathematically.

For both light and material particles there are basic relationships between energy and frequency, and between momentum and wavelength, which are summarised in the following formulae:

Light	Matter
$E = h\nu$	$E = h\nu = \hbar\omega$
$p = \dfrac{h\nu}{c}$	$p = \dfrac{h}{\lambda} = \hbar k$.

(7.1)

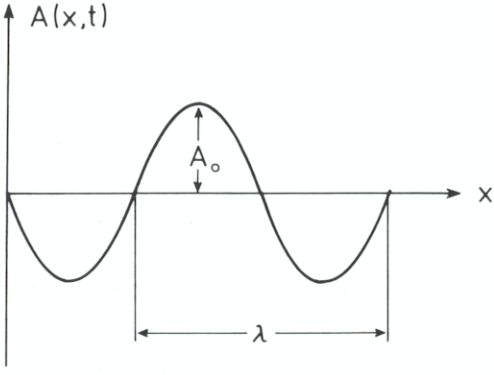

Fig. 7.1. Instantaneous view of a wave with amplitude A_0 and wavelength λ

We now wish to expand these relationships into a more exact theory. We are familiar with descriptions of wave motion from the study of light. If we consider a plane monochromatic wave (Fig. 7.1) travelling in the x direction, the wave amplitude A at time t and point x is $A(x,t) = A_0 \cos(kx - \omega t)$. The wave number k is related to the wavelength λ by $k = 2\pi/\lambda$. The circular frequency ω is related to the frequency by $\omega = 2\pi\nu$. In many cases it is more useful to use complex notation, in which we express the cosine by exponential functions according to the formula

$$\cos\alpha = \tfrac{1}{2}(e^{i\alpha} + e^{-i\alpha}) . \tag{7.2}$$

We accordingly expand $A(x,t)$:

$$A(x,t) = A_0 \tfrac{1}{2}[\exp(\mathrm{i}kx - \mathrm{i}\omega t) + \exp(-\mathrm{i}kx + \mathrm{i}\omega t)] . \tag{7.3}$$

Applying the relations (7.1), we obtain

$$\exp(\mathrm{i}kx - \mathrm{i}\omega t) = \exp\left[\frac{\mathrm{i}}{\hbar}(px - Et)\right] . \tag{7.4}$$

The wave represented by (7.4) is an infinitely long wave train.

On the other hand, since we ordinarily assume that particles ("point masses") are localised, we must consider whether we can, by superposing a sufficient number of suitable wave trains, arrive at some spatially concentrated sort of "wave". We are tempted to form what are called *wave packets*, in which the amplitude is localised in a certain region of space. In order to get an idea of how such wave packets can be built up, we first imagine that two wave trains of slightly differing frequencies and wavenumbers are superposed. We then obtain from the two amplitudes $A_1(x,t)$ and $A_2(x,t)$ a new amplitude $A(x,t)$ according to

$$A(x,t) = A_1(x,t) + A_2(x,t) , \tag{7.5}$$

or, using cosine waves of the same amplitude for A_1 and A_2,

$$A(x,t) = A_0[\cos(k_1 x - \omega_1 t) + \cos(k_2 x - \omega_2 t)] . \tag{7.6}$$

As we know from elementary mathematics, the right-hand side of (7.6) may be expressed as

$$2A_0 \cos(kx - \omega t) \cos(\Delta k x - \Delta\omega t) , \tag{7.7}$$

where

$$k = \tfrac{1}{2}(k_1 + k_2) , \qquad \omega = \tfrac{1}{2}(\omega_1 + \omega_2) ,$$

and

$$\Delta k = \tfrac{1}{2}(k_1 - k_2) , \qquad \Delta\omega = \tfrac{1}{2}(\omega_1 - \omega_2) .$$

The resulting wave is sketched in Fig. 7.2. The wave is clearly amplified in some regions of space and attenuated in others. This suggests that we might produce a more and more complete localisation by superposing more and more cosine waves. This is, in fact, the case. To see how, we use the complex representation. We superpose waves of the form (7.4) for various wavenumbers k and assume that the wavenumbers form a continuous distribution. Thus, we form the integral

$$\int_{k_0 - \Delta k}^{k_0 + \Delta k} a \exp[\mathrm{i}(kx - \omega t)]\, dk = \psi(x,t) , \tag{7.8}$$

where a is taken to be a constant amplitude.

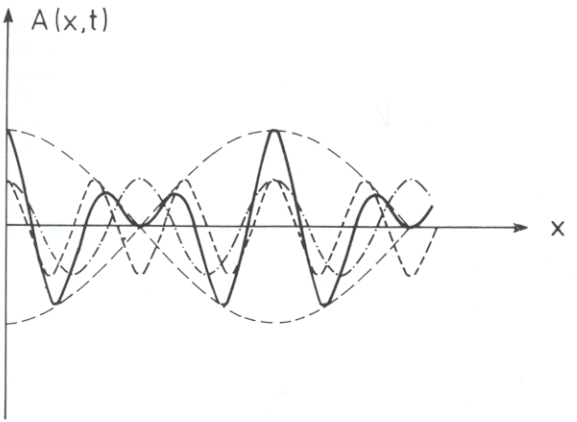

Fig. 7.2. Superposition of two waves of the same amplitude. Fundamental wave 1: $(-\cdot-)$, fundamental wave 2: $(--)$ same amplitude as 1. Resulting wave A: (——). The envelope $\cos(\Delta k x - \Delta\omega t)$ for constant t is also shown as a dashed curve

In taking this integral, we must notice that ω and k are related to one another, since the energy and the momentum of an electron are connected by the relation $E = p^2/(2m_0)$, and this in turn means that ω and k are related according to (7.1). To evaluate the integral we set

$$k = k_0 + (k - k_0) \tag{7.9}$$

and expand ω about the value k_0 using a Taylor series in $(k - k_0)$, which we terminate after the second term:

$$\omega = \omega_0 + \left(\frac{d\omega}{dk}\right)(k - k_0) + \dots \,. \tag{7.10}$$

In the following, we abbreviate $d\omega/dk$ as ω'. Inserting (7.9) and (7.10) in (7.8), we obtain

$$\psi(x,t) = a\exp[-\mathrm{i}(\omega_0 t - k_0 x)] \int_{-\Delta k}^{\Delta k} \exp[-\mathrm{i}(\omega' t - x)\,\xi]\, d\xi\,, \tag{7.11}$$

where we have set $(k - k_0) = \xi$. The remaining integral may be evaluated in an elementary manner and (7.11) finally takes the form

$$\psi(x,t) = a\exp(-\mathrm{i}\,\omega_0 t + \mathrm{i}\,k_0 x) \cdot 2\,\frac{\sin[(\omega' t - x)\,\Delta k]}{\omega' t - x}\,. \tag{7.12}$$

The real part of ψ is shown in Fig. 7.3.

We can draw two important conclusions from (7.12):

1) The wave packet represented by ψ is strongly localised in the region of $x = \omega' t$. The maximum amplitude moves with a velocity $\omega' \equiv d\omega/dk$. With the help of (7.1), we can express ω and k in terms of E and p, obtaining $\omega' = \partial E/\partial p$, or, if we use the standard relation $E = p^2/2m_0$, finally $\omega' = p/m_0 = v_{\text{particle}}$. In order to understand this result, we recall the concepts of phase velocity and group velocity.

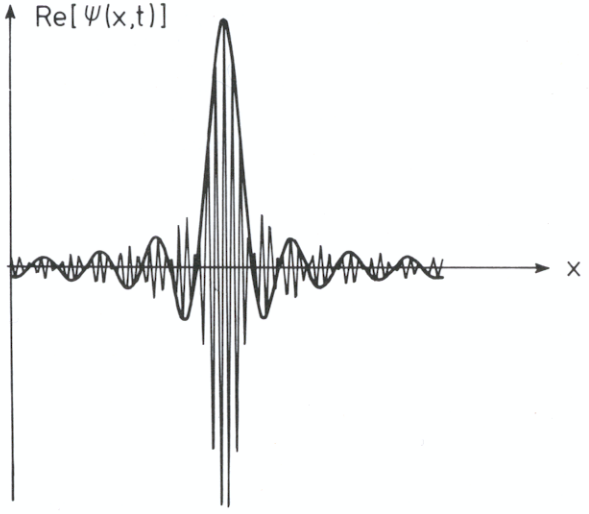

Fig. 7.3. The real part of $\psi(x,t)$ as a function of the position x. The rapid oscillations are described by $\cos(k_0 x - \omega_0 t)$ with t fixed. The envelope is given by $\sin[(\omega' t - x)\Delta k]/(\omega' t - x)$ with t fixed. Note that the scale of the x axis has been greatly reduced in comparison to Fig. 7.2

If we let the time variable increase in the wavefunction $\cos(kx - \omega t)$, then the position $x_{\max}$ at which a particular wave maximum is to be found moves according to the relation $kx_{\max} - \omega t = 0$, i.e. $x_{\max} = (\omega/k)t$. The position $x_{\max}$ thus moves with the *phase velocity* $v_{\text{phase}} = \omega/k$.

If we replace ω by E and k by p according to (7.1), we find immediately that this v does *not* equal the particle velocity. On the other hand, we have just seen that the maximum of a *wavepacket* moves with the velocity $v_G = d\omega/dk$. This velocity of a wave group (wavepacket) is called the *group velocity*. Thus the group velocity of the de Broglie waves (matter waves) is identical with the particle velocity.

We could be tempted to unify the wave and particle pictures by using wave packets to describe the motion of particles. This is unfortunately not possible, because in general, wave packets change their shapes and flow apart with time. We are therefore compelled to adopt a quite different approach, as will be shown below.

2) A second implication of the result (7.12) is the following: The width of a wave packet is roughly the distance between the first two zero points to the left and right of

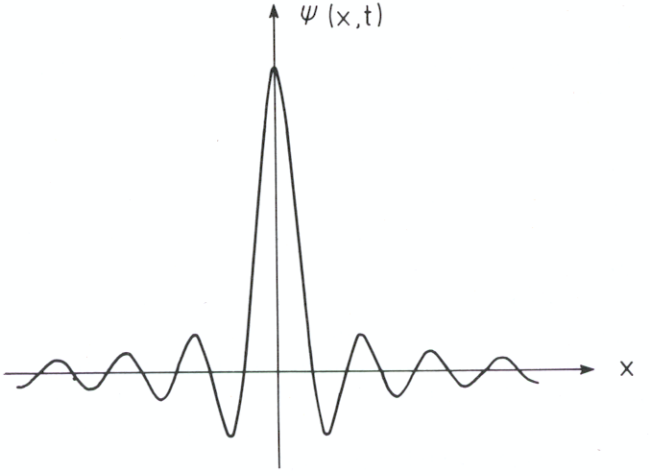

Fig. 7.4. The envelope of the real part of the wave packet (7.12) (Fig. 7.3). The first node is at $x_0 = \pi/\Delta k$

the maximum (Fig. 7.4). Since the first zero point is at $x_0 = \pi/\Delta k$, the width of the wave packet would be $\Delta x = 2\pi/\Delta k$. The more we wish to concentrate the wave packet, i.e., the smaller we make Δx, the larger we must make the k-region, or Δk.

In order to clarify the relationship between the particle and the wave descriptions, we shall consider the experiment described in the following section as we have already for light.

7.2 Probabilistic Interpretation

We wish to illustrate, using the electron as an example, how one can unify the wave and particle descriptions. To determine the position of an electron in the x direction (Fig. 7.5), we allow an electron beam to pass through a slit with a width Δx. We can thus ensure that the electron coming from the left must have passed through this position. Now, however, the wave properties come into play, and the electron is accordingly diffracted by the slit. A diffraction pattern is produced on the screen S (Fig. 7.5). According to wave theory, the intensity of the diffraction pattern is proportional to the square of the amplitude. When we consider the electron as a wave, and take ψ as its wave amplitude, we obtain the intensity $I = |\psi(x,t)|^2$ at time t and position x on the observation screen. It is better, for both mathematical and physical reasons, not to speak of the intensity at a *point* in space, but rather of the intensity in the three-dimensional region dx, dy, dz around the point x, y, z.

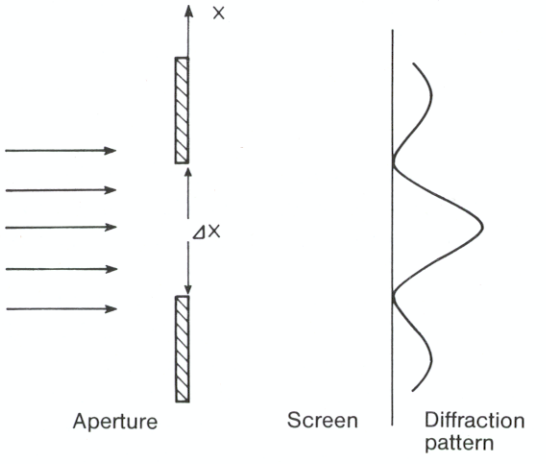

Fig. 7.5. An electron beam (*arrows at left*) passes through an aperture and generates a diffraction pattern on a screen. The intensity distribution on the screen is shown schematically on the right

Therefore, in the following we shall consider the intensity in a volume element $dV = dx\,dy\,dz$:

$$I\,dx\,dy\,dz = |\psi(x,y,z,t)|^2 dx\,dy\,dz\,. \tag{7.13}$$

(Compare this to the one-dimensional example in Fig. 7.6.)

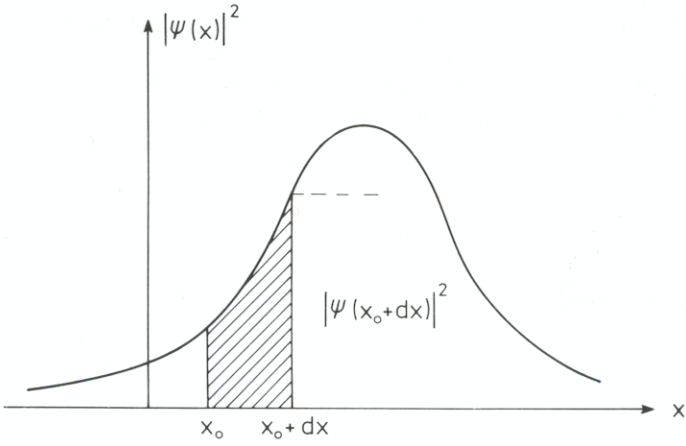

Fig. 7.6. $|\psi(x)|^2$ as a function of x at a given time t. The shaded area corresponds to the probability that the electron is located in the interval x_0 to x_0+dx

Now comes the essential point. The screen can also be considered as an apparatus which detects electrons individually as particles. A fluorescent screen flashes at the point of impact each time an electron hits it. The electron is thus highly localised, and there is no diffraction pattern. If we repeat the experiment, we observe other flashes of light, and in general these are at different points on the screen. Only when we carry out many experiments, or allow many electrons to pass through, do we obtain a diffraction pattern of the form described by (7.13). This is the key to the explanation of the phenomenon of "wave-particle duality". On the one hand, the intensity of the diffraction pattern in a volume ΔV is proportional to the absolute square of the amplitude,

$$|\psi|^2 \Delta V , \tag{7.14}$$

and on the other, it is proportional to the probability of finding the electron in ΔV. $|\psi|^2 \Delta V$ is thus itself proportional to the frequency of finding the electron in ΔV. $|\psi(x,y,z,t)|^2 dx\,dy\,dz$ must therefore be seen as the *probability* of finding the electron in a volume element dV about the point x,y,z.

Because the statistical interpretation of quantum mechanics will be mentioned frequently, and is absolutely necessary to an understanding of the subject, we shall spend a bit more time on the concept of probability. Let us compare a quantum mechanical experiment with a game of dice. Since a die has six different numbers on its faces, it has, so to speak, six different experimental values. We cannot say in advance, however, which face, i.e. which experimental value we will obtain in any given throw. We can only give the probability P_n of obtaining the value n. In the case of a die, P_n is very easy to determine. According to a basic postulate of probability theory, the sum of all probabilities P_n must be one (i.e., one face must come up on each throw):

$$\sum_n P_n = 1 . \tag{7.15}$$

Since all the numbers $n = 1, 2, \ldots 6$ are equally probable, the six values of P_n must be equal, so $P_n = 1/6$.

It is not so easy to determine $|\psi|^2 dx\,dy\,dz$. We can infer from the above, however, that there must be a normalisation condition for $|\psi|^2 dx\,dy\,dz$. If we integrate over all points in space, the particle must be found *somewhere*, so the total probability must therefore be equal to 1. We thereby obtain the basic normalisation condition

$$\int |\psi(x,y,z)|^2 dx\,dy\,dz = 1\,. \tag{7.16}$$

We shall illustrate the use of this normalisation condition with two examples.

1) We assume that the electron is enclosed in a box with volume V. The integral (7.16) must then extend only over this volume. If we use for ψ the wavefunction

$$\psi = A_0 \exp(\mathrm{i}\boldsymbol{k}\cdot\boldsymbol{x} - \mathrm{i}\omega t)\,, \tag{7.17}$$

where $\boldsymbol{k}\cdot\boldsymbol{x} = k_x x + k_y y + k_z z$, then A_0 must be

$$A_0 = V^{-1/2}\,. \tag{7.18}$$

2) If the space extends to infinity, there is a difficulty, because here $A_0 = 0$ if we simply allow V to go to infinity in (7.18). It can be shown, however, that a generalised normalisation condition can still be derived. In one dimension the normalised wavefunction is

$$\psi_k(x,t) = (1/\sqrt{2\pi}) \exp(\mathrm{i}kx - \mathrm{i}\omega t)\,, \tag{7.19}$$

and the normalisation condition is

$$\int \psi_k^*(x,t)\,\psi_{k'}(x,t)\,dx = \delta(k-k')\,. \tag{7.20}$$

Here $\delta(k-k')$ is the Dirac δ function (see Appendix A).

The probabilistic interpretation of the wavefunction is also necessary for the following reason: if the impact of an electron on the screen were to cause it to flash at more than one point, this would mean that the electron had divided itself. All experiments have shown, however, that the electron is *not* divisible. The determination of $|\psi|^2 dV$ allows us only to predict the probability of finding the electron in that volume. If we have found it at one position (localised it), we are certain that it is not somewhere else as well. This is evidently a "yes-no" statement and leaves no ambiguity for an individual electron. If we consider the reflection of electrons in this way, and observe that 5% are reflected, it means this: if we carry out a very large number of experiments, 5% of all the electrons would be reflected. It would be completely false, however, to say that 5% of a single electron had been reflected.

7.3 The Heisenberg Uncertainty Relation

We now consider some of the implications of the fact that the electron sometimes acts as a particle and sometimes as a wave. As we calculated earlier, the one-dimensional distribution of the wave packet is

$$\psi(x) \sim \frac{\sin(x\,\Delta k)}{x}\,. \tag{7.21}$$

If we take the position of the first zero point as a measure of the uncertainty in the position, we obtain from (7.21) (Fig. 7.4) the relation

$$\frac{\Delta x}{2} = \frac{\pi}{\Delta k}. \tag{7.22}$$

The uncertainty in the position is clearly connected with the uncertainty in the wavenumbers k. But the wavenumber is related to the momentum by the equation

$$p = \hbar k. \tag{7.23}$$

If we insert this in (7.22), we obtain the basic Heisenberg uncertainty relation

$$\Delta x \Delta p \geqq h \tag{7.24}$$

(a mathematically precise formulation and derivation can be found in Appendix C). This relation states that it is impossible to measure the position and the momentum of an electron exactly at the same time. A lower bound to the simultaneous measurability is given by (7.24). Indeed, if we wished to let Δx go to zero (exact determination of the position), we would have to allow Δp to become infinite, and *vice versa*. The fact that we notice nothing of this uncertainty relation in daily life is a result of the smallness of Planck's constant h. If, on the other hand, we consider the microscopic world, then we can only understand the results of experiments if we take the finite size of the constant h into account. We will clarify the meaning of (7.24) with the example of an experiment.

An electron is moving in a horizontal direction (y). We wish to determine its coordinate in the perpendicular (x) direction. For this purpose, we set up a collimator perpendicular to the direction of motion with a slit of width $d = \Delta x$. If the electron passes through this slit, then we know that it was at that position with the uncertainty Δx. Now, however, we must take into account the wave nature of the electron. From the theory of diffraction we know that a wave produces a diffraction pattern on the obser-

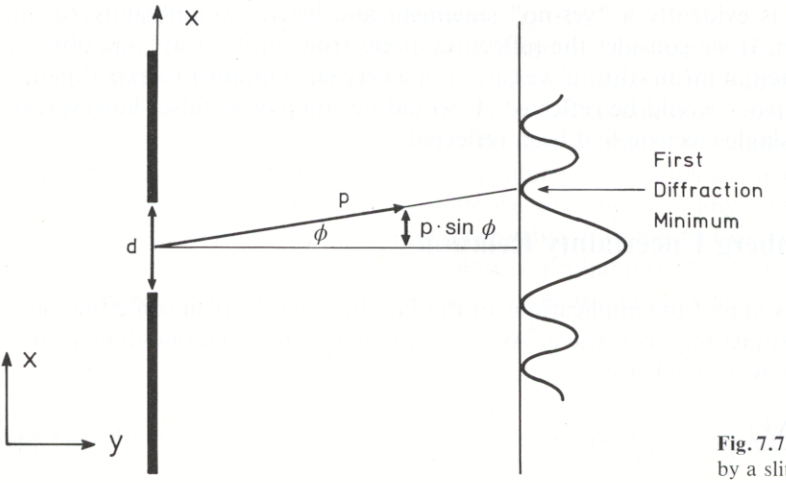

Fig. 7.7. Diffraction of a wave by a slit

vation screen after passing through a slit of width d (Fig. 7.7). The angle ϕ at which the first diffraction minimum occurs is given by

$$\sin\phi = \lambda/d\,. \tag{7.25}$$

If we denote the total momentum of the electron by $\boldsymbol{p}$, the projection of the momentum on the x axis is $p\sin\phi$. This x component in the momentum is produced by diffraction of the electron wave at the slit; the resulting uncertainty in the momentum is then

$$\Delta p_x = p\sin\phi\,. \tag{7.26}$$

If we once again use the relation

$$p = h/\lambda \tag{7.27}$$

and insert (7.26) and (7.27) in (7.25), we again obtain the Heisenberg uncertainty relation (7.24).

This example shows clearly that a measurement of one quantity, here the position, immediately produces a perturbation of the complementary quantity, namely the momentum. Before we set up the collimator with its slit, we could have determined the momentum of the electron. The result would have been that the electron was moving exactly in the y direction, i.e., that its momentum component in the x direction was exactly equal to zero. In the above experiment, we were able to determine the position with a certain accuracy, but we had to accept the fact that the momentum thereby became uncertain in the x direction. There is also a relation between energy and time which is analogous to (7.24).

7.4 The Energy-Time Uncertainty Relation

In the wavefunction $\sim\exp(\mathrm{i}kx - \mathrm{i}\omega t)$, which was the starting point of this chapter, the position x and the time t occur in a symmetric fashion. Just as we could form wave packets which exhibited a certain concentration in space, we can also construct wave packets which have a concentration about a time t with an uncertainty Δt. Instead of the relation $\Delta x\Delta k \geqq 2\pi$, we then have

$$\Delta t\Delta\omega \geqq 2\pi\,. \tag{7.28}$$

Utilising the relation $E = \hbar\omega$, we find from this that

$$\Delta E\Delta t \geqq h\,. \tag{7.29}$$

This relation, which we shall discuss in more detail at a later point in the book, states among other things, that one must carry out a measurement for a sufficiently long time, in order to measure an energy with good accuracy in quantum mechanics.

7.5 Some Consequences of the Uncertainty Relations for Bound States

In the preceding sections of this chapter we have explicitly considered *free* electrons. In the next chapters we shall be concerned with the experimental and theoretical questions associated with *bound* electrons, for example in the hydrogen atom. In this section we shall to some extent anticipate the presentation in the rest of the book. The reader will recognise even in this section that wave mechanics will play a fundamental role in the treatment of bound states.

We will consider the hydrogen atom as the simplest case of a bound state. We assume that the electron travels around the nucleus in an orbit, as a planet around the sun. Why the electronic shells of the atom have a finite extent – why there is a smallest electron orbit – was an insoluble problem in classical physics.

The energy of an electron is equal to the sum of the kinetic and the potential energy,

$$E_{\text{class}} = E_{\text{kin}} + E_{\text{pot}} . \tag{7.30}$$

If we express the kinetic energy of a particle $E_{\text{kin}} = (m_0/2)\, v^2$ in terms of the momentum p, and substitute the Coulomb potential energy $-e^2/(4\pi\varepsilon_0 r)$ for E_{pot}, the expression for E is

$$E = \frac{p^2}{2m_0} - \frac{e^2}{4\pi\varepsilon_0 r} . \tag{7.31}$$

Here r is the distance of the electron from the nucleus.

It can be shown in classical mechanics that $E_{\text{class}} = -e^2/(2 \cdot 4\pi\varepsilon_0 r)$.

If we allow r to go to zero, the energy naturally goes to $-\infty$. In other words, the energy decreases continually and there is no smallest orbital radius. Let us now consider the expression (7.31) from a "naive" quantum mechanical point of view. Then "orbit" would mean that we have the electron concentrated at a distance of approximately r from the nucleus. The positional uncertainty would therefore be of the order of r. This, however, would entail uncertainty in the momentum p of the order of h/r, which in turn establishes a minimum for the order of magnitude of the kinetic energy (Fig. 7.8). If we therefore substitute

$$p \approx \frac{h}{r} \tag{7.32}$$

in (7.31), we realise that the minimum of the energy expression

$$E = \frac{1}{2m_0} \frac{\mathrm{h}^2}{r^2} - \frac{e^2}{4\pi\varepsilon_0 r} = \text{Min} \tag{7.33}$$

is no longer at $r = 0$. If we let r go to zero, the kinetic energy would increase very rapidly. We shall leave the determination of the minimum of (7.33) to the reader as an simple exercise in differential calculus and give the result immediately. The radius is

$$r = \frac{h^2 4\pi\varepsilon_0}{m_0 e^2} . \tag{7.34}$$

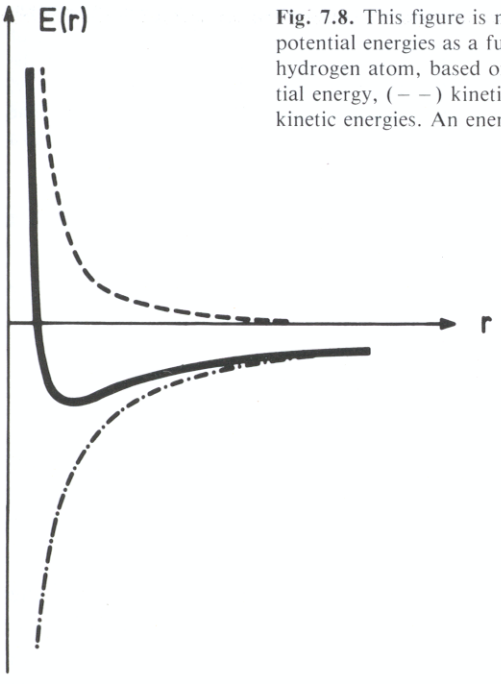

Fig. 7.8. This figure is meant to clarify the competition between kinetic and potential energies as a function of the distance $r \leftrightarrow$ position uncertainty in the hydrogen atom, based on the Heisenberg uncertainty relation. ($-\cdot-$) potential energy, ($- -$) kinetic energy, (——) total energy = sum of potential and kinetic energies. An energy minimum is seen to result

If we substitute this r in (7.33), the corresponding energy is

$$E = -\frac{1}{2}\frac{e^4 m_0}{(4\pi\varepsilon_0)^2 \hbar^2}. \tag{7.35}$$

When we substitute the known numerical values for Planck's constant, and the mass and charge of the electron, we obtain a radius of about 10^{-8} cm, which is the right order of magnitude for the hydrogen atom. As we shall see later, the exact quantum mechanical calculation of the energy yields

$$E = -\frac{1}{2}\frac{e^4 m_0}{(4\pi\varepsilon_0)^2 \hbar^2}. \tag{7.36}$$

The only difference between (7.35) and (7.36) is the factor $\hbar^2 \equiv (h/2\pi)^2$ which replaces h^2.

The Heisenberg uncertainty principle also allows us to calculate the so-called *zero-point energy of a harmonic oscillator.* Here we consider the motion of a particle elastically bound by a spring with a spring constant f. Since the elastic energy increases quadratically with the displacement x and the kinetic energy again has the form $p^2/2m_0$, the total energy is

$$E = \frac{p^2}{2m_0} + \frac{f}{2}x^2. \tag{7.37}$$

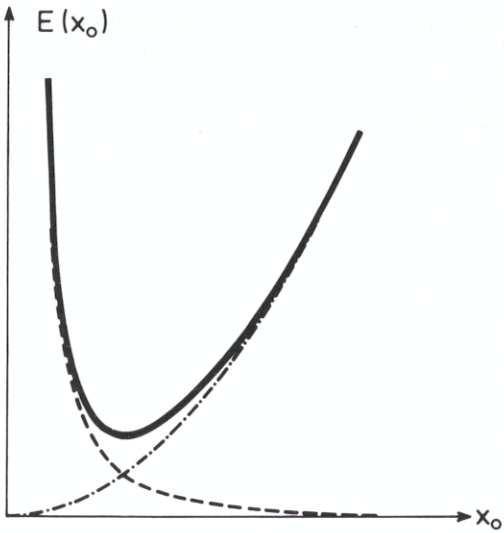

Fig. 7.9. Illustrating the competition between kinetic and potential energies as a function of the displacement ↔ position uncertainty in the harmonic oscillator. (– · –) potential energy, (– –) kinetic energy, (——) total energy. The classical energy minimum at $x_0 = 0$ is shifted to a finite value

In classical physics this energy is at a minimum when both the momentum and the position are zero, i.e., the particle is at rest. However, since according to the Heisenberg relation an exact position is associated with an infinite momentum, we allow a positional uncertainty of the same magnitude as the oscillation amplitude x_0 and have the corresponding momentum uncertainty according to (7.24), where x_0 assumes the role of r (Fig. 7.9). We again require that the total energy is minimised by the appropriate choice of x_0:

$$E = \frac{h^2}{2m_0 x_0^2} + \frac{f}{2} x_0^2 = \text{Min} . \tag{7.38}$$

Solving this equation for x_0 yields the amplitude of the harmonic oscillator,

$$x_0 = \sqrt[4]{\frac{h^2}{m_0 f}} . \tag{7.39}$$

The energy then has the form

$$E = h\omega . \tag{7.40}$$

As we shall see later, an exact quantum mechanical calculation yields the relations

$$E = \tfrac{1}{2}\hbar\omega \tag{7.41}$$

and

$$x_0 = \sqrt{\frac{\hbar}{2m_0\omega}} . \tag{7.42}$$

It follows from these considerations that atomic, elastically bound particles are fundamentally incapable of being at rest. Such elastically coupled particles occur, for example, in crystal lattices. The quantum theory predicts that these atoms will constantly carry out zero-point oscillations.

Problems

7.1 Normalise the wave packet

$$\psi(x,t) = N \int_{-\infty}^{+\infty} \exp\left[-\frac{k^2}{2(\Delta k)^2} \right] e^{i[kx-\omega(k)t]} dk$$

for $t = 0$. Then calculate $\psi(x,t)$ for a free particle of mass m_0 for $t > 0$. Does the normalisation hold for $t > 0$? On the basis of the occupation probability, decide whether the wave packet falls apart. What is the significance of

$$\exp\left(-\frac{k^2}{2(\Delta k)^2} \right) ?$$

Hint: Use the relation

$$\int_{-\infty}^{+\infty} e^{-a\xi^2 - b\xi} d\xi = e^{b^2/(4a)} \int_{-\infty}^{+\infty} e^{-a[\xi + b/(2a)]^2} d\xi$$

(completing the square!)

The second integral can be converted to the Gaussian integral by changing the coordinates.

7.2 By the appropriate choice of Δk in Problem 7.1, let the probability of locating the wave packet outside $\Delta x = 10^{-8}$ cm be zero. How long would it take Δx to attain the size of the distance between the earth and sun ($\simeq$150 million km)?

Hint: Choose Δx so that $\psi(\Delta x, 0) = 1/e$ [$e \equiv \exp(1)$!]

7.3 Treat Problems 7.1 and 7.2 in three dimensions.

8. Bohr's Model of the Hydrogen Atom

8.1 Basic Principles of Spectroscopy

In the following chapters we shall take up the detailed analysis of the spectra of atoms in every wavelength region. The most important sources of information about the electronic structure and composition of atoms are spectra in the visible, infrared, ultraviolet, x-ray, microwave and radio frequency ranges. Figure 8.1 summarises these spectral regions.

Optical spectra are further categorised as line, band and continuous spectra. Continuous spectra are emitted by radiant solids or high-density gases. Band spectra consist of groups of large numbers of spectral lines which are very close to one another. They are generally associated with molecules. Line spectra, on the other hand, are typical of atoms. They consist of single lines, which can be ordered in characteristic series.

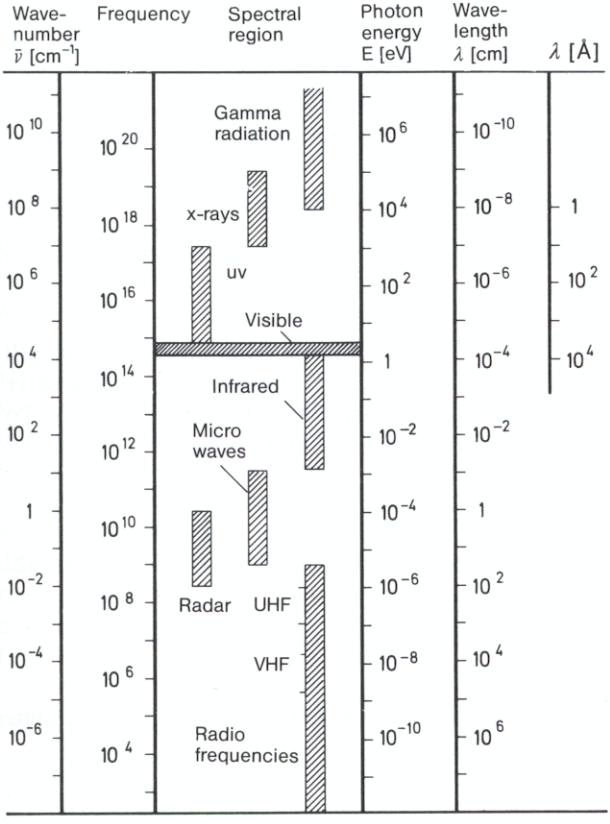

Fig. 8.1. The electromagnetic spectrum. Regions and units

Optical spectra can be observed either by emission or by absorption. The former mode requires that the substance to be examined be made to emit light; this can be achieved by transferring energy to the atoms by means of light, electron collisions, x-ray excitation or some other process. If a substance re-emits the light it has absorbed, the process is called resonance fluorescence. The best known example of this is the resonance fluorescence of sodium vapour (Fig. 8.2).

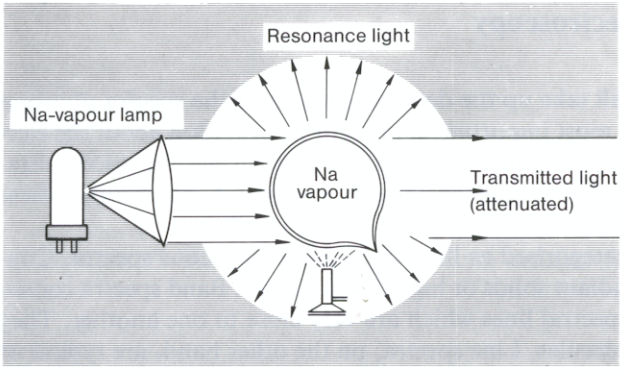

Fig. 8.2. Resonance fluorescence of sodium vapour. Sodium metal is heated in an evacuated glass sphere. The resulting sodium vapour absorbs the light of a sodium vapour lamp and emits the same light as resonance fluorescence in all directions

Details of apparatus will be discussed in the following sections in connection with particular problems.

Spectra are traditionally measured in several different units, due to the features of the apparatus or for practical reasons:

– In *wavelength* units. These can be determined absolutely with a diffraction grating. Usually, however, one uses a calibrated comparison spectrum, which allows greater accuracy.

One wavelength standard is the yellow ^{86}Kr line, that is a yellow line in the spectrum of the ^{86}Kr atom. For this line,

$$\lambda_{\text{vac}} = 6057.80211\ \text{Å} \triangleq \bar{\nu} = 16507.6373\ \text{cm}^{-1} \quad \text{(see below)}\,.$$

In general the wavelengths are referred to vacuum. The corresponding wavelength in air is somewhat smaller, because the index of refraction of air is somewhat greater than 1, and the velocity of light in air is thus somewhat less than in a vacuum. To convert wavelengths measured in air ("normal" air, 15 °C, 760 Torr), the formula is

$$\lambda_{\text{air}} = \lambda_{\text{vac}}/n\,.$$

The refractive index of air is a function of the wavelength. At 6000 Å, $n = 1.0002762$.

For the yellow ^{86}Kr line in normal air,

$$\lambda_{\text{air}} = 6056.12941\ \text{Å}\,.$$

– Specifying the *frequency* is more general, since it is not dependent on the medium. We have:

$$\nu = c/\lambda_{\text{vac}} = c/(n\lambda_{\text{air}})\,.$$

– A frequently cited quantity is the *wavenumber*:

$$\bar{\nu} = \nu/c = 1/\lambda_{\text{vac}} = 1/(n\lambda_{\text{air}}) .$$

The wavenumber is, like the frequency, a quantity proportional to the energy; conversion may be made according to the equation

$$E = \bar{\nu} h c .$$

– Finally, the unit *electron volt* (eV) is often used as a measure of the energy.

Several units which are important and practical in atomic physics as well as conversion factors are set out in Table 8.1 and in Fig. 8.1.

Table 8.1. Frequently used units and conversion factors (see also the table on the inner side of the front cover)

Quantity	Unit and conversion factor
Wavelength λ	$1\ \text{Å} = 10^{-10}\ \text{m} = 0.1\ \text{nm}$
Wavenumber $\bar{\nu}$	$1\ \text{cm}^{-1}$ (= 1 kayser)
$\bar{\nu} = 1/\lambda$	$\bar{\nu} = 8066\ E(\text{eV})\ \text{cm}^{-1}$
	$1\ \text{cm}^{-1} = 29.979\ \text{GHz}$
Energy E	$1\ \text{electron volt} = 1.602 \cdot 10^{-19}\ \text{J} = 1.96 \cdot 10^{-6}\ m_0 c^2$
	$E = h\nu = hc/\lambda = hc\bar{\nu}$
	$1\ \text{eV} \triangleq 2.418 \cdot 10^{14}\ \text{Hz} \triangleq 8066\ \text{cm}^{-1}$
	$E(\text{eV}) = 1.24 \cdot 10^{-4}\ \dfrac{\bar{\nu}}{\text{cm}}$
Mass m_0	$1\ \text{electron mass} = 9.11 \cdot 10^{-31}\ \text{kg} = 511\ \text{keV}/c^2$
Charge e	$1\ \text{elementary charge} = 1.6 \cdot 10^{-19}\ \text{C}$
Planck's constant h	$h = 4.14 \cdot 10^{-15}\ \text{eV s}$
	$\hbar = h/2\pi = 6.58 \cdot 10^{-16}\ \text{eV s}$

8.2 The Optical Spectrum of the Hydrogen Atom

Kirchhoff and *Bunsen*, the founders of spectroscopic analysis, were the first to discover in the mid-19th century that each element possesses its own characteristic spectrum. Hydrogen is the lightest element, and the hydrogen atom is the simplest atom, consisting of a proton and an electron. The spectra of the hydrogen atom have played an important rôle again and again over the last 90 years in the development of our understanding of the laws of atomic structure and of the structure of matter.

The emission spectrum of atomic hydrogen shows three characteristic lines in the visible region at 6563, 4861, and 4340 Å ($H_{\alpha,\beta,\gamma}$). The most intense of these lines was discovered in 1853 by Ångström; it is now called the H_α line. In the near ultraviolet region, these three lines are followed by a whole series of further lines, which fall closer and closer together in a regular way as they approach a short-wavelength limit (H_∞) (Fig. 8.3).

Balmer found in 1885 that the wavelengths of these lines could be extremely well reproduced by a relation of the form

$$\lambda = \left(\frac{n_1^2}{n_1^2 - 4}\right) G . \qquad (8.1)$$

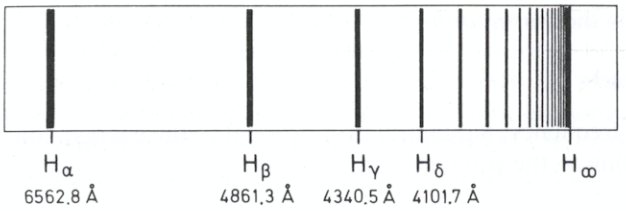

Fig. 8.3. Balmer series in the hydrogen emission spectrum. The convergence of the lines to the series limit H_∞ is clearly seen

Here n_1 is an integer, $n_1 = 3, 4, \ldots$ and G is an empirical constant. Today, we write the Balmer formula somewhat differently. For the wavenumbers of the lines we write

$$\bar{\nu} = 1/\lambda = R_H\left(\frac{1}{2^2} - \frac{1}{n^2}\right), \qquad n \text{ an integer } > 2 \tag{8.2}$$

The quantity $R_H(=4/G)$ is called the *Rydberg constant* and has the numerical value

$$R_H = 109677.5810\ \text{cm}^{-1}.$$

The series limit is found for $n \to \infty$ to be

$$\bar{\nu}_\infty = R_H/4.$$

For the further investigation of the hydrogen spectrum, astrophysical observations have played an important rôle. In the spectra of stars, photographically recorded as early as 1881 by *Huggins*, a large number of lines from the hydrogen spectrum are seen.

Table 8.2. The first 20 lines of the Balmer series of hydrogen. The numbers quoted are wavelengths in air, the wavenumbers in vacuum, and the values calculated from the Balmer formula

n	λ_{air} [Å]	$\bar{\nu}_{vac}$ [cm^{-1}]	$R_H\left(\frac{1}{2^2} - \frac{1}{n^2}\right)$
H_α 3	6562.79	15233.21	15233.00
H_β 4	4861.33	20564.77	20564.55
H_γ 5	4340.46	23032.54	23032.29
H_δ 6	4101.73	24373.07	24372.80
H_ε 7	3970.07	25181.33	25181.08
H_ζ 8	3889.06	25705.84	25705.68
H_η 9	3835.40	26065.53	26065.35
H_ϑ 10	3797.91	26322.80	26322.62
H_ι 11	3770.63	26513.21	26512.97
H_κ 12	3750.15	26658.01	26657.75
H_λ 13	3734.37	26770.65	26770.42
H_μ 14	3721.95	26860.01	26859.82
H_ν 15	3711.98	26932.14	26931.94
H_ξ 16	3703.86	26991.18	26990.97
H_o 17	3697.15	27040.17	27039.89
H_π 18	3691.55	27081.18	27080.88
H_ϱ 19	3686.83	27115.85	27115.58
H_σ 20	3682.82	27145.37	27145.20

Using modern radio-astronomical techniques, transitions between states with extremely large n-values have been found; levels with n between 90 and 350 could be identified.

The reason that many lines were discovered first in astrophysical observations and not by experiments on the earth is connected with the difficulty of preparing pure atomic hydrogen in the laboratory. Gas discharges, in which H_2 gas is decomposed into atomic hydrogen and excited to fluorescence, always contain fluorescing hydrogen molecules as well, whose spectrum overlaps the atomic-hydrogen spectrum.

Above the series limit we observe the so-called series-limit continuum, a region in which the spectrum shows no more lines, but is, instead, continuous.

A comparison of the calculated spectral lines obtained from the Balmer formula (8.2) with the observed lines (Table 8.2) shows that the formula is not just a good approximation: the series is described with great precision. The whole spectrum of the H atom is represented by equations of the form

$$\bar{\nu} = R_H \left(\frac{1}{n'^2} - \frac{1}{n^2} \right) \quad \text{with } n' < n \text{ being integers .} \tag{8.3}$$

The numbers n and n' are called *principal quantum numbers*. Table 8.3 contains some of the lines from the first four series.

Table 8.3. The wavelengths of some lines of the various spectral series in hydrogen. The series with $n' = 5$ was observed in 1924 by *Pfund*; it begins with a line of $\lambda = 74000$ Å, but is not shown in the table

n \ n'	1 *Lyman*	2 *Balmer*	3 *Paschen*	4 *Brackett*
2	1216 Å ≙ 82257 cm^{-1}			
3	1026 Å ≙ 97466 cm^{-1}	6563 Å ≙ 15233 cm^{-1}		
4	973 Å ≙ 102807 cm^{-1}	4861 Å ≙ 20565 cm^{-1}	18751 Å ≙ 5333 cm^{-1}	
5	950 Å ≙ 105263 cm^{-1}	4340 Å ≙ 23033 cm^{-1}	12818 Å ≙ 7801 cm^{-1}	40500 Å ≙ 2467 cm^{-1}
Year of discovery	1906	1885	1908	1922

The relation (8.3) was formulated first by *Rydberg* in 1889. He found, "to his great joy", that the Balmer formula (8.1) is a special case of the Rydberg formula (8.3). Table 8.3 also illustrates the Ritz Combination Principle, which was found empirically in 1898. It states:

The difference of the frequencies of two lines in a spectral series is equal to the frequency of a spectral line which actually occurs in another series from the same atomic spectrum. For example, the frequency difference of the first two terms in the Lyman series is equal to the frequency of the first line of the Balmer series, as can be seen from the wavenumber entries in Table 8.3.

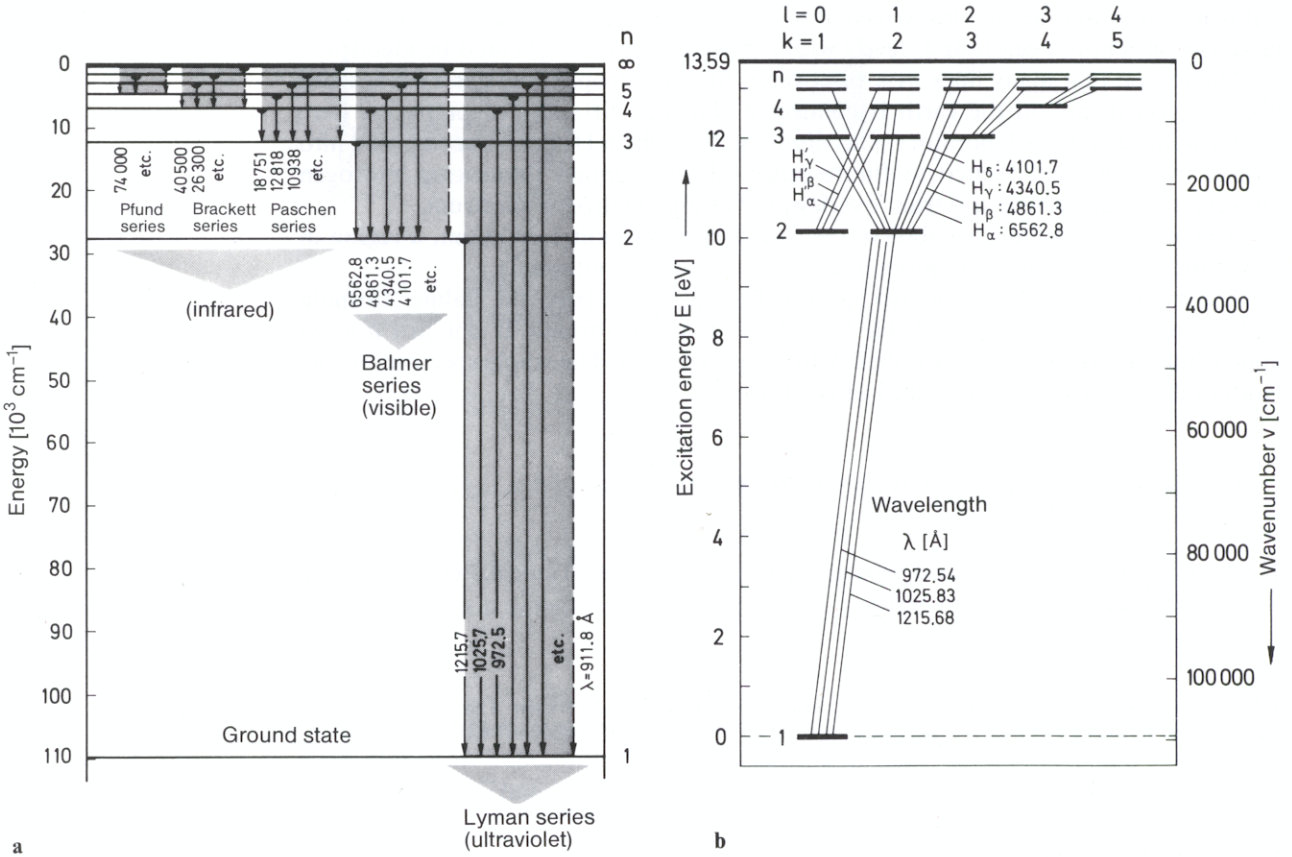

Fig. 8.4. a) Term diagram of the lines of the hydrogen spectrum and series classification. The wavelengths of the transitions are given in Å. The energies can be given as (negative) binding energies, with the zero of energy being the ionisation limit, or they can be given as excitation energies, beginning with the ground state, so that the energy of the term n_∞ is equal to the ionisation energy **b)** This represents the lines of the hydrogen spectrum in the term scheme of *Grotrian* [Struktur der Materie VII (Springer, Berlin 1928)]. The symbols l and k appearing in the upper margin of the figure will be explained later (Sect. 8.9)

We can conclude from observation and inductive reasoning that the frequencies (or wavenumbers) of all the spectral lines can be represented as differences of two *terms* of the form R/n^2. As we shall see in the following, these are just the energy levels of the electron in a hydrogen atom. The spectral lines of the hydrogen atom can be graphically pictured as transitions between the energy levels (terms), leading to a spectral *energy level diagram* (Fig. 8.4).

8.3 Bohr's Postulates

In the early years of this century, various models were suggested to explain the relationship between atomic structure and the spectral lines. The most successful of these is due to *Bohr* (1913). Following the Rutherford model, he assumed that the electrons move around the nucleus in circular orbits of radius r with velocity v, much as the planets move around the sun in the Solar System. A dynamic equilibrium between the cen-

trifugal force and the Coulomb attraction of the electrons to the nucleus is assumed to exist. Thus, for the hydrogen atom, one has

$$\frac{e^2}{4\pi\varepsilon_0 r^2} = m_0 r\omega^2 . \tag{8.4}$$

The corresponding energy is the sum of the kinetic and the potential energies of the electrons:

$$E = E_{\text{kin}} + E_{\text{pot}} ,$$

where the kinetic energy, as usual, is given by $m_0 v^2/2$ or $m_0 r^2\omega^2/2$. The potential energy is defined as the work which one obtains on allowing the electron to approach the nucleus under the influence of the Coulomb force from infinity to a distance r. Since the work is defined as the product of force and distance, and the Coulomb force changes continuously with the distance from the nucleus, we must integrate the contributions to the work along a differential path dr; this gives

$$E_{\text{pot}} = \int_{\infty}^{r} \frac{e^2}{4\pi\varepsilon_0 r'^2}\, dr' = -\frac{e^2}{4\pi\varepsilon_0 r} . \tag{8.5}$$

E_{pot}, as a binding energy, may be seen to be negative, with the zero point being the state of complete ionisation. The total energy is thus found to be

$$E = \frac{1}{2} m_0 r^2\omega^2 - \frac{e^2}{4\pi\varepsilon_0 r} . \tag{8.6}$$

Thus far, the model corresponds to that of *Rutherford*.

We may rewrite (8.6) by using (8.4):

$$E = -\frac{e^2}{2\cdot 4\pi\varepsilon_0 r} = -\frac{1}{2(4\pi\varepsilon_0)^{2/3}} (e^4 m_0\omega^2)^{1/3} . \tag{8.7}$$

If, however, one attempts to understand the emission and absorption of light using this model and the known laws of classical electrodynamics, one encounters fundamental difficulties. *Classically*, orbits of arbitrary radius and thus a *continuous* series of energy values for the electron in the field of the nucleus should be allowed. But on identifying the energy levels which are implied by the spectral series with the values of the electron's energy, one is forced to assume that only *discrete* energy values are possible. Furthermore, electrons moving in circular orbits are accelerated charges, and as such, they should radiate electromagnetic waves with frequencies equal to their orbital frequencies, $\nu = \omega/2\pi$. They would thus lose energy continuously, i.e. their orbits are unstable and they would spiral into the nucleus. Their orbital frequencies would change continuously during this process. Therefore, the radiation emitted would include a continuous range of frequencies.

In order to avoid this discrepancy with the laws of classical physics, *Bohr* formulated three *postulates* which describe the deviations from classical behavior for the electrons in an atom. These postulates proved to be an extremely important step towards quantum mechanics. They are:

- The classical equations of motion are valid for electrons in atoms. However, only certain *discrete* orbits with the energies E_n are allowed. These are the energy levels of the atom.
- The motion of the electrons in these quantised orbits is *radiationless*. An electron can be transferred from an orbit with lower (negative) binding energy E_n (i.e. larger r) to an orbit with higher (negative) binding energy $E_{n'}$, (smaller r), emitting radiation in the process. The frequency of the emitted radiation is given by

$$E_n - E_{n'} = h\nu . \tag{8.8}$$

Light absorption is the reverse process.

By comparing (8.8) and (8.3), *Bohr* identified the energy terms $E_{n'}$ and E_n as

$$E_n = -\frac{Rhc}{n^2}, \quad E_{n'} = -\frac{Rhc}{n'^2}, \tag{8.9}$$

where the minus sign again implies that we are dealing with binding energies.

- Finally, for the calculation of the Rydberg constant R in (8.9) from atomic quantities, *Bohr* used the comparison of the orbital frequencies of the electrons with the frequency of the emitted or absorbed radiation. In classical physics, these frequencies would be equal, as mentioned above. However, using (8.4), one can easily calculate that this is not at all the case in the hydrogen atom for small orbital radii r.

Bohr's decisive idea was then to postulate that with increasing orbital radius r, the laws of quantum atomic physics become identical with those of classical physics. The application of this *"Correspondence Principle"* to the hydrogen atom allows the determination of the discrete stable orbits.

We consider the emission of light according to the first two postulates for a transition between neighboring orbits, i.e. for $(n-n') = 1$, and for large n. From (8.3) we have for the frequency ν, with $n - n' = \tau$

$$\nu = Rc\left(\frac{1}{n'^2} - \frac{1}{n^2}\right) = Rc\left(\frac{1}{(n-\tau)^2} - \frac{1}{n^2}\right) \tag{8.10}$$

$$Rc\frac{1}{n^2}\left(\frac{1}{(1-\tau/n)^2} - 1\right) \cong Rc\frac{2\tau}{n^3}$$

or, with $\tau = 1$,

$$\nu = \frac{2Rc}{n^3} . \tag{8.11}$$

This frequency is now set equal to the classical orbital frequency $\omega/2\pi$ in (8.7), setting (8.7) equal to (8.9) and inserting in (8.11); this yields an equation from which R can be calculated:

$$\frac{Rhc}{n^2} = \frac{1}{2}\frac{1}{(4\pi\varepsilon_0)^{2/3}}\left[e^4 m_0 \left(\frac{2\pi 2Rc}{n^3}\right)^2\right]^{1/3}$$

and

$$R = \frac{m_0 e^4}{8\varepsilon_0^2 h^3 c} . \tag{8.12}$$

From (8.12), we find for the Rydberg constant R (which we denote by R_∞ for reasons which will become apparent below) the numerical value

$$R_\infty = (109\,737.318 \pm 0.012)\ \mathrm{cm}^{-1}\,. \tag{8.13}$$

This may be compared with the empirical value in (8.2). In *Bohr's* model, R is just the ionisation energy of the ground state of the atom, $n = 1$.

From (8.12), with (8.7) and (8.9), we find the radius r_n of the nth orbital to be

$$r_n = \frac{n^2 \hbar^2 4\pi\varepsilon_0}{e^2 m_0}\,. \tag{8.14}$$

The quantum number n which occurs in these expressions is called the *principal quantum number.*

In addition, we may calculate the *orbital angular momentum* $\boldsymbol{l} = \boldsymbol{r} \times \boldsymbol{p}$ of an electron having velocity v_n and orbital frequency ω_n in the orbit with radius r_n and find, using (8.11) and (8.14), the quantisation rule

$$|\boldsymbol{l}| = m_0 v_n r_n = m_0 r_n^2 \omega_n = n\hbar \quad \text{with} \quad n = 1, 2, 3, \ldots\,. \tag{8.15}$$

This quantisation rule is often (but incorrectly) taken to be one of *Bohr's* postulates.

The essential common feature of the Bohr postulates is that they make no statements about processes, but only about states. The classical orbital concept is abandoned. The electron's behaviour as a function of time is not investigated, but only its stationary initial and final states. Figure 8.5 illustrates the model.

Whether spectral lines are observable, either in emission or in absorption, depends on the occupation of the energy terms (also referred to as energy states). Absorption from a state presupposes that this state is occupied by an electron. In emission transitions, an electron falls from a higher state into an unoccupied lower one; the electron must be previously raised to the higher state by an excitation process, i.e. by an input of energy. At normal temperatures only the Lyman series in hydrogen is observable in absorption, since then only the lowest energy term ($n = 1$ in Fig. 8.4) is occupied. When the Balmer lines are observed in the spectra of stars as Fraunhofer lines (that is, these

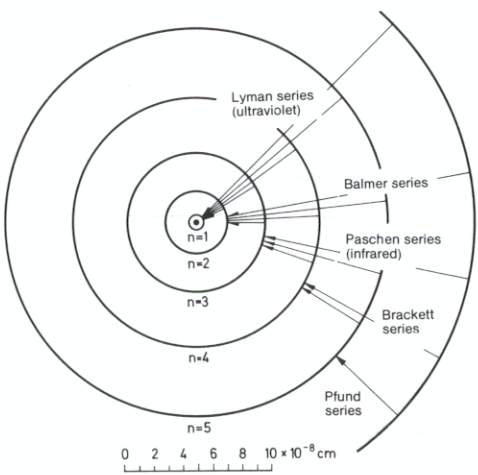

Fig. 8.5. Schematic representation of the Bohr atomic model, showing the first five spectral series

lines are missing in the continuous spectrum because of absorption of light on the way through the stellar atmosphere), then it can be concluded that the temperature of the atmosphere is so high, that the first excited state of the H atom ($n = 2$) is also occupied. This is the basis of spectroscopic temperature determination utilising the Boltzmann distribution (2.8). For example, in the sun, with a surface temperature of 6000 K, only 10^{-8} of the hydrogen atoms in the solar atmosphere are in the $n = 2$ state.

8.4 Some Quantitative Conclusions

We will now treat the Bohr model with arbitrary nuclear charge for *hydrogen-like* systems such as He^+, Li^{2+}, etc. quantitatively. The nucleus with charge Z is orbited by an electron in a circular orbit n at a distance r_n and with the velocity v_n. There is an equilibrium between the Coulomb force and the centrifugal force:

$$\frac{Ze^2}{4\pi\varepsilon_0 r_n^2} = \frac{m_0 v^2}{r_n} = m_0 r_n \omega_n^2, \tag{8.16}$$

where $\omega_n = v_n/r_n$ is the circular frequency of the electron in its orbit n and m_0 is its mass. For the possible orbital radii follows, see (8.14)

$$r_n = \frac{n^2\hbar^2 4\pi\varepsilon_0}{Ze^2 m_0}. \tag{8.17}$$

With $Z = 1$, $n = 1$ we find for the smallest orbital radius r_1 in the hydrogen atom $r_1(\mathrm{H}) = 0.529$ Å, the right order of magnitude for the spatial extension of the neutral hydrogen atom. $r_1(\mathrm{H})$ is referred to as the *Bohr radius* of the hydrogen atom in the ground state, abbreviated a_0.

For the possible circular frequencies of the electronic motion we obtain

$$\omega_n = \frac{1}{(4\pi\varepsilon_0)^2}\,\frac{Z^2 e^4 m_0}{n^3\hbar^3}. \tag{8.18}$$

For $Z = 1$, $n = 1$, the largest possible circular frequency is seen to be

$$\omega_1(\mathrm{H}) \cong 10^{16}\,\mathrm{Hz};$$

ω_n would be the "classical" frequency of the emitted light if the electron behaved like a classical dipole in the atom. This is, however, not the case, see Sect. 8.3. The emitted frequency corresponds to the *difference* of the energy states of two orbits n and n' according to (8.9). The total energy is according to (8.6)

$$E_n = m_0 v_n^2/2 - \frac{Ze^2}{4\pi\varepsilon_0 r_n}. \tag{8.19}$$

Substituting for r_n from (8.17) and v_n, which can be obtained from (8.15), yields the possible energy states:

$$E_n = -\frac{Z^2 e^4 m_0}{32\pi^2 \varepsilon_0^2 \hbar^2} \cdot \frac{1}{n^2} . \tag{8.20}$$

For $Z = 1$, $n = 1$ we find the lowest energy state of the hydrogen atom:

$$E_1(\mathrm{H}) = -13.59\ \mathrm{eV} .$$

This is the ionisation energy of the H atom.

For arbitrary Z, $n = 1$, one obtains

$$E_1(Z) = -Z^2 \cdot 13.59\ \mathrm{eV} .$$

For the wavenumbers of the spectral lines we find, according to (8.3) and (8.9)

$$\bar{\nu} = \frac{1}{hc}(E_n - E_{n'}) = \frac{e^4 m_0 Z^2}{64\pi^3 \varepsilon_0^2 \hbar^3 c}\left(\frac{1}{n'^2} - \frac{1}{n^2}\right) . \tag{8.21}$$

Comparison of this result with the empirically found Balmer formula (see Sect. 8.2) shows complete agreement with respect to the quantum numbers n and n'. The quantum number n which was introduced by *Bohr* is thus identical with the index n of the Balmer formula.

8.5 Motion of the Nucleus

The spectroscopically measured quantity R_H (Sect. 8.2) does not agree exactly with the theoretical quantity R_∞ (8.13). The difference is about $60\ \mathrm{cm}^{-1}$. The reason for this is the motion of the nucleus during the revolution of the electron, which was neglected in the above model calculation. This calculation was made on the basis of an infinitely massive nucleus; we must now take the finite mass of the nucleus into account.

In mechanics it can be shown that the motion of two particles, of masses m_1 and m_2 and at distance r from one another, takes place around the common centre of gravity. If the centre of gravity is at rest, the total energy of both particles is that of a fictitious particle which orbits about the centre of gravity at a distance r and has the mass

$$\mu = \frac{m_1 m_2}{m_1 + m_2} , \tag{8.22}$$

referred to as the *reduced mass*. In all calculations of Sect. 8.4 we must therefore replace the mass of the orbiting electron, m_0, by μ and obtain, in agreement with experiment,

$$R = R_\infty \frac{1}{1 + m_0/M} . \tag{8.23}$$

Here $m_0 \equiv m_1$, the mass of the orbiting electron, and $M \equiv m_2$, the mass of the nucleus. The energy corrections due to motion of the nucleus decrease rapidly with increasing nuclear mass (Table 8.4).

Table 8.4. Energy correction for motion of the nucleus for the Rydberg numbers of several one-electron atoms

Atom	$H(^1H)$	$D(^2H)$	$T(^3H)$	He^+	Li^{2+}
A	1	2	3	4	7
$-\frac{\Delta E}{E} \cdot 10^4$	5.45	2.75	1.82	1.36	0.78
$-\frac{\Delta E}{E}$ %	0.0545	0.0275	0.0182	0.0136	0.0078

This observation makes possible a spectroscopic determination of the mass ratio M/m_0, e.g.

$$M_{\text{proton}}/m_{\text{electron}} = 1836.15 .$$

Due to the motion of the nucleus, different isotopes of the same element have slightly different spectral lines. This so-called isotope displacement led to the discovery of heavy hydrogen with the mass number $A = 2$ (deuterium). It was found that each line in the spectrum of hydrogen was actually double. The intensity of the second line of each pair was proportional to the content of deuterium. Figure 8.6 shows the H_β line with the accompanying D_β at a distance of about 1 Å in a 1 : 1 mixture of the two gases. The nucleus of deuterium contains a neutron in addition to the proton. There are easily measurable differences in the corresponding lines of the H and D Lyman series, namely

$$R_H = R_\infty \cdot \frac{1}{1 + m_0/M_H} = 109677.584 \text{ cm}^{-1}, \tag{8.24}$$

$$R_D = R_\infty \cdot \frac{1}{1 + m_0/M_D} = 109707.419 \text{ cm}^{-1}. \tag{8.25}$$

The difference in wavelengths $\Delta\lambda$ for corresponding lines in the spectra of light and heavy hydrogen is:

$$\Delta\lambda = \lambda_H - \lambda_D = \lambda_H \left(1 - \frac{\lambda_D}{\lambda_H}\right) = \lambda_H \left(1 - \frac{R_H}{R_D}\right). \tag{8.26}$$

Fig. 8.6. β lines of the Balmer series in a mixture of equal parts hydrogen (^1H) and deuterium (^2H). One sees the isotope effect, which is explained by motion of the nucleus. The lines are about 1 Å apart and have the same intensity here, because the two isotopes are present in equal amounts [from K. H. Hellwege: *Einführung in die Physik der Atome*, Heidelberger Taschenbücher, Vol. 2, 4th ed. (Springer, Berlin, Heidelberg, New York 1974) Fig. 40a]

Table 8.5 gives the measured values. The agreement between the calculated and measured values is excellent.

Historical remark: a difference of about 0.02% had been found between the values of the molecular weight of hydrogen determined chemically and by mass spectroscopy, because D is present in the natural isotopic mixture of hydrogen. Its mass was included in the results obtained by chemical means, but not by mass spectroscopy. In 1931, however, *Urey* discovered spectral lines which, according to their Rydberg number, belonged to D by observing a gas discharge through the vapour of 3 litres of liquid hydrogen evaporated into a 1 cm^3 volume (Fig. 8.6).

Table 8.5. Comparison of the wavelengths of corresponding spectral lines in hydrogen and deuterium. The lines belong to the Lyman series

λ_D/Å	λ_H/Å
1215.31	1215.66
1025.42	1025.72
972.25	972.53

8.6 Spectra of Hydrogen-like Atoms

According to *Bohr*, the spectra of all atoms or ions with only one electron (one-electron systems) should be the same except for the factor Z^2 and the Rydberg number. The spectrum of hydrogen should thus explain those of the ions He^+, Li^{2+}, Be^{3+} or any other ions which have only one electron. This has been completely verified experimentally (see Table 8.6 and the energy diagram in Fig. 8.7).

For He^+, astronomers found the Fowler series

$$\bar{\nu}_F = 4R_{He}\left(\frac{1}{3^2} - \frac{1}{n^2}\right) \tag{8.27}$$

Table 8.6. Wavelengths λ_{12} of the first Lyman lines, i.e. the spectral lines with $n' = 1$, $n = 2$, of hydrogen and hydrogen-like atomic ions. The mass correction (*first column*) is used to calculate the Rydberg number (*second column*) and thus λ_{12} (*third column*). The calculated values are in good agreement with the measured values (*fourth column*)

	$1 + \frac{m_0}{m_{nucl}}$	R_{nucl} [cm^{-1}]	λ_{12} (calc) [Å]	λ_{12} (meas) [Å]
^1H	1.00054447	109677.6	1215.66	1215.66
^2H	1.00027148	109707.4	1215.33	1215.33
$^4He^+$	1.00013704	109722.3	303.8	303.6
$^7Li^{2+}$	1.00007817	109728.7	135.0	135.0
$^9Be^{3+}$	1.00006086	109730.6	75.9	75.9
$^{10}B^{4+}$	1.00005477	109731.3	48.6	48.6
$^{11}B^{4+}$	1.00004982	109731.8		
$^{12}C^{5+}$	1.00004571	109732.3	33.7	33.7

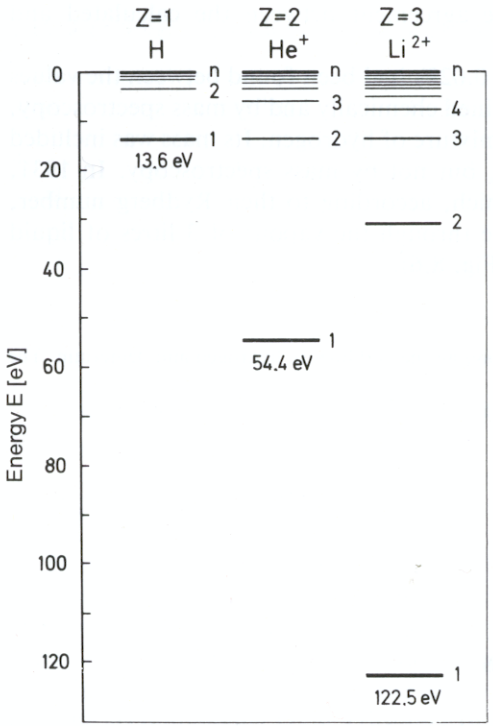

Fig. 8.7. Some energy levels of the atoms H, He^+ and Li^{2+}

Table 8.7. Comparison of the spectral lines of the Balmer series in hydrogen and the Pickering series in the helium ion, in Å

He^+	H
6560.1	6562.8 (H_α)
5411.6	
4859.3	4861.3 (H_β)
4561.6	
4338.7	4340.5 (H_γ)
4199.9	
4100.0	4101.7 (H_δ)

and the Pickering series

$$\bar{\nu}_P = 4R_{He}\left(\frac{1}{4^2} - \frac{1}{n^2}\right), \tag{8.28}$$

which can also be represented as

$$\bar{\nu}_P = R_{He}\left(\frac{1}{2^2} - \frac{1}{(n/2)^2}\right), \quad n = 5, 6 \ldots . \tag{8.29}$$

Every other line of the Pickering series thus almost corresponds to one of the Balmer lines of H. This is shown in Table 8.7.

Later other He^+ series were found, such as the

1st Lyman series $$\bar{\nu}_{L1} = 4R_{He}\left(\frac{1}{1^2} - \frac{1}{n^2}\right), \tag{8.30}$$

2nd Lyman series $$\bar{\nu}_{L2} = 4R_{He}\left(\frac{1}{2^2} - \frac{1}{n^2}\right). \tag{8.31}$$

For Li^{2+}, Be^{3+} and still heavier highly ionised atoms, spectral lines have been observed which can be calculated by multiplying the frequencies of the lines of the

H atom by Z^2 and insertion of the corresponding Rydberg constant. With increasing nuclear charge Z, we quickly reach the region of x-ray wavelengths.

In 1916, the collected spectroscopic experience concerning the hydrogen-similarity of these spectra was generalised in the *displacement theorem* of *Sommerfeld* and *Kossel*, which states:

The spectrum of any atom is very similar to the spectrum of the singly charged positive ion which follows it in the periodic table.

Hydrogen-like heavy atoms, i.e. heavy atoms from which all the electrons except one have been removed, can be prepared by accelerating the singly-ionised atoms to high energies and passing them through a thin foil; their electrons are "stripped off" on passing through the foil. For example, in order to strip all the electrons from a uranium atom and produce U^{92+} ions, they must be accelerated to energies greater than 10 GeV. By permitting the U^{92+} ions to recapture one electron each, one can then obtain the hydrogen-like ion U^{91+}. The corresponding spectral lines are emitted as the captured electron makes transitions from orbits of high n to lower orbits. For U^{91+}, the Lyman series has been observed in the spectral region around 100 keV and the Balmer series is in the region between 15 and 35 keV (Th. Stöhlker, Phys. Bl. **52**, 42 (1996)).

8.7 Muonic Atoms

With the simple Bohr model, the muonic atoms, first observed in 1952, can be described. They contain, instead of an electron, the 207-times heavier μ meson or muon and are, in contrast to the Rydberg atoms, extremely small, in extreme cases hardly larger than the typical diameter of an atomic nucleus.

To produce them, matter is bombarded with energetic protons (about 440 MeV), giving rise to other elementary particles, the pions, according to the following reaction schemes:

$$p+n\rightarrow n+n+\pi^+ \quad \text{or} \quad p+n\rightarrow p+p+\pi^- .$$

Here p denotes the proton, n the neutron, and π the pion.

Pions have a charge $+e$ or $-e$ and mass $m_\pi = 273\, m_0$. They decay into other particles, the muons, according to the reactions

$$\pi^+\rightarrow\mu^+ + \nu_\mu \quad \text{or} \quad \pi^-\rightarrow\mu^- + \bar{\nu}_\mu .$$

Here, the symbols ν or $\bar{\nu}$ mean a neutrino or an antineutrino, the index μ means muon neutrino (neutretto), and electron neutrinos carry the index e to distinguish them. The neutrinos are only shown for completeness.

The half-life for this decay is $T_{1/2} = 2.5 \cdot 10^{-8}$ s. Muons may be characterised as heavy electrons; they have a charge e, a mass equal to $206.8\, m_0$, and a half-life $T_{1/2} = 2.2 \cdot 10^{-6}$ s.

Muons decay into electrons (e^-) or into positrons (e^+) according to the reactions

$$\mu^+\rightarrow e^+ + \nu_e + \bar{\nu}_\mu , \quad \mu^-\rightarrow e^- + \bar{\nu}_e + \nu_\mu .$$

Before they decay, they can be captured into outer atomic orbits by atomic nuclei and can occupy these orbits in the place of electrons. In making transitions from the outer

to inner orbits, the muons radiate light of the corresponding atomic transition frequency; this is light in the x-ray region of the spectrum. Since muons behave like heavy electrons, we can simply apply the results of the Bohr model. For the orbital radii we have, see (8.17)

$$r_n = \frac{4\pi\varepsilon_0\hbar^2}{Ze^2 m_\mu} n^2 . \tag{8.32}$$

r_n is thus smaller than the radius of the corresponding orbit which is occupied by an electron by the ratio of the electron to the muon mass.

A numerical example: for the magnesium atom ^{12}Mg we find

$$\text{Electron:} \quad r_1(e^-) = \frac{0.53}{12}\,\text{Å} = 4.5 \cdot 10^{-12}\,\text{m} ,$$

$$\text{Muon:} \quad r_1(\mu^-) = \frac{r_1(e^-)}{207} = 2.2 \cdot 10^{-14}\,\text{m} .$$

The muon is thus much closer to the nucleus than the electron. For the radiation from a transition between the levels with principal quantum numbers 1 and 2 the following expression holds:

$$h\nu = \frac{Z^2 e^4 m_\mu}{32\pi^2\varepsilon_0^2\hbar^2}\left(\frac{1}{1^2} - \frac{1}{2^2}\right), \tag{8.33}$$

that is, the quantum energy is larger by the ratio of the masses than the energy of the corresponding transition in an electronic atom. Finally, the muon decays as described above, or else it is captured by the nucleus, which then may itself decay.

Muonic atoms are observed for the most part by means of the x-radiation which they emit; this radiation decays in intensity with the half-life characteristic of muons. Muonic atoms are interesting objects of nuclear physics research. Since the muons approach the nucleus very closely, much more so than the electrons in an electronic atom, they can be used to study details of the nuclear charge density distribution, the

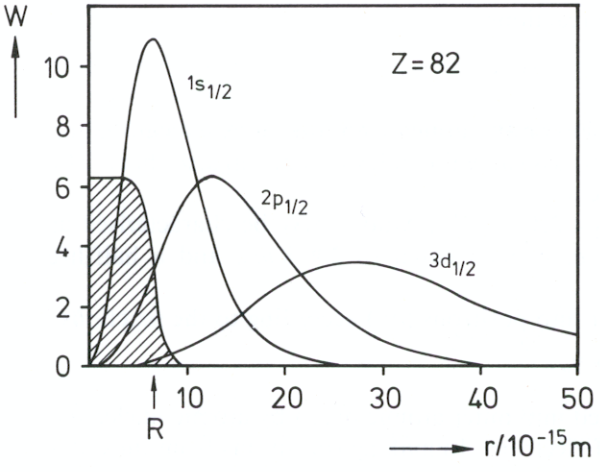

Fig. 8.8. The probability W of finding a muon at a distance r from the center of the nucleus of a muonic atom, in arbitrary units, for various shells; also showing the nuclear charge distribution (*shaded area*). The plot is for the lead nucleus, with $Z = 82$ and nuclear radius $R = 6.687 \cdot 10^{-15}$ m (fm). The symbols used to indicate the shells will be explained later. (After E. Boric and G.A. Rinker: Rev. Mod. Phys. **54**, 68 (1982))

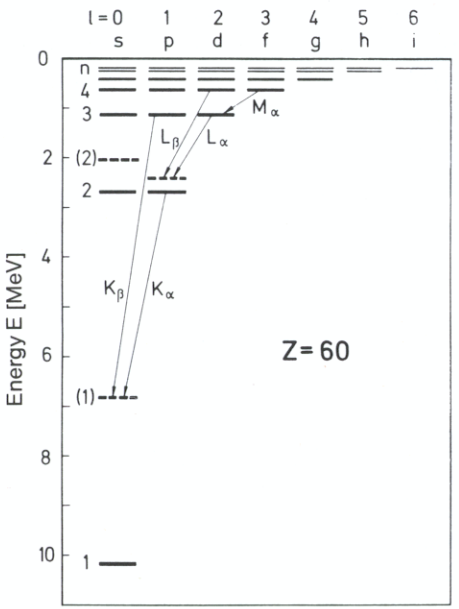

▲ **Fig. 8.9.** Muonic terms for an atom with $Z = 60$. The fully drawn levels correspond to the assumption of a point nucleus; the dashed levels take account of the finite nuclear size. The notation used for the transitions corresponds to that used for x-ray lines (Chap. 18). Note the energy scale

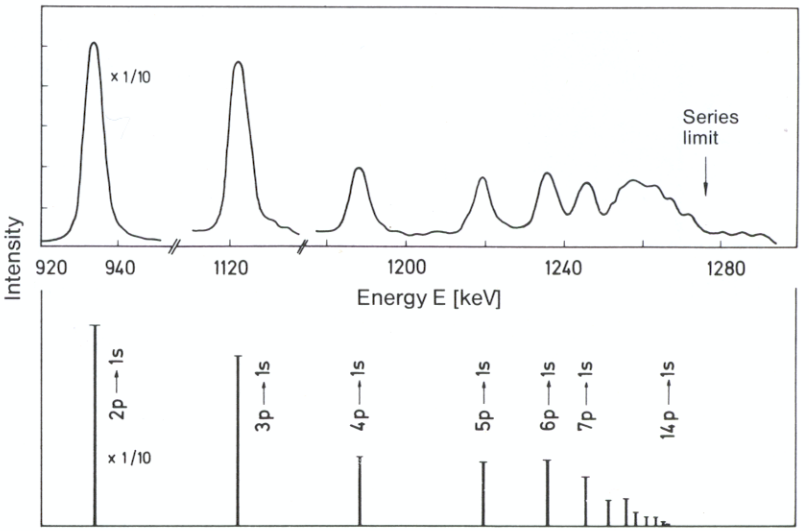

▲ **Fig. 8.10.** Lyman series ($np \rightarrow 1s$) of the muonic transitions in a titanium atom. Note the energy scale

distribution of the nuclear magnetic moment within the nuclear volume and of nuclear quadrupole deformation.

Figure 8.8 shows the spatial distribution of a muon in several orbits of a lead atom. It can be seen that the muons in these orbits spend a considerable amount of time in the nucleus or in its immediate neighbourhood. Since the muons approach the nuclear charge Ze very closely, the binding and excitation energies become extremely large.

Figure 8.9 shows a term diagram of the muonic-atom levels for a nuclear charge number $Z = 60$. The analogy with the hydrogen atom is evident; however, the transitions here are in the energy region of MeV, i.e. in the region of hard x-rays and of gamma rays. For the investigation of such muonic atoms, one therefore requires the tools of nuclear physics. Detection of the radiation is carried out with scintillator or solid-state detectors.

Finally, Fig. 8.10 shows an example of the measurement of radiation from a muonic atom, the Lyman series in the muonic spectrum of titanium. The notations s, p, d, etc. in Figs. 8.8–10 refer to the orbital angular momentum of the electrons (muons). They will be further described in Sect. 8.9.

8.8 Excitation of Quantum Jumps by Collisions

Lenard investigated the ionisation of atoms as early as 1902 using electron collisions. For his measurements, he used an arrangement following the principle of the experimental scheme shown in Fig. 8.11. The free electrons produced by thermionic emission are accelerated by the positive grid voltage V_G and pass through the open-meshed grid into the experimental region. Between the grid and the plate A at the right of the drawing, which serves as the third electrode, a plate voltage V_A is applied. The plate is

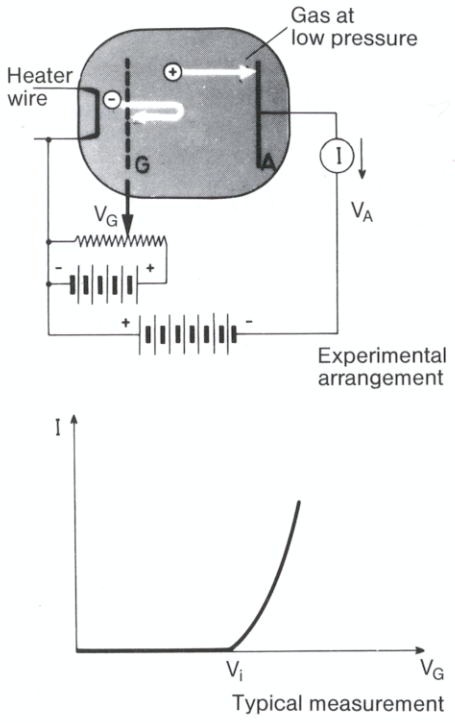

Fig. 8.11. Experimental arrangement for detecting ionisation processes in gases. Only positive ions, which are formed by collisions with electrons, can reach the plate A. In the lower part of the figure, the plate current is plotted as a function of the grid voltage V_G. V_i is the voltage with which the electrons must be accelerated in order to be able to ionise the atoms

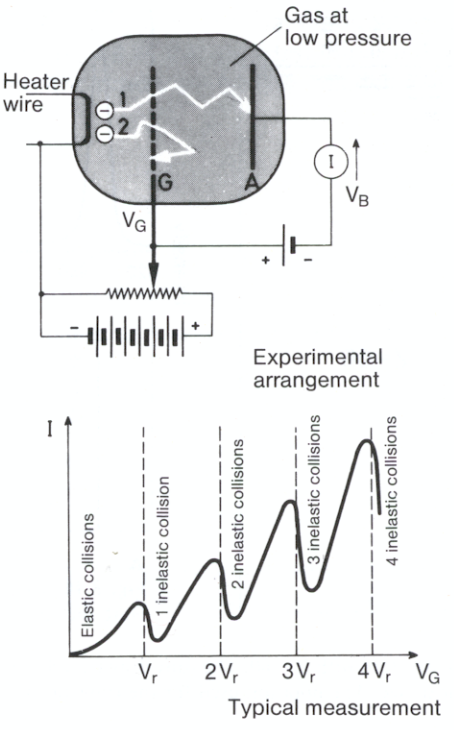

Fig. 8.12. Experimental arrangement of *Franck* and *Hertz* for investigating inelastic collisions between electrons and atoms. Electrons on the way from the grid to the anode can transfer their kinetic energies partially (particle 1) or completely (particle 2) to the gas atoms. The anode current as a function of the grid voltage is plotted in the lower part of the figure. At high grid voltages, several energy-transfer processes can occur one after the other

negatively charged relative to the grid. The voltages are chosen so that the electrons cannot reach the plate; they pass through the grid and are repelled back to it. When an electron has ionised an atom of the gas in the experimental region, however, the ion is accelerated towards the plate A. Ionisation events are thus detected as a current to the plate.

The current is plotted as a function of the grid voltage V_G in the lower part of Fig. 8.11. Only when the electrons have a certain minimum energy eV_i does the current appear. The corresponding accelerating potential V_i is the ionisation potential of the atoms.

Franck and *Hertz* showed for the first time in 1913 that the existence of discrete energy levels in atoms can be demonstrated with the help of electron collision processes independently of optical-spectroscopic results. Inelastic collisions of electrons with atoms can result in the transfer of amounts of energy to the atoms which are smaller than the ionisation energy and serve to excite the atoms without ionising them.

The experimental setup is shown schematically in Fig. 8.12. Electrons from a heated cathode are accelerated by a variable voltage V_G applied to a grid. They pass through the grid and are carried by their momenta across a space filled with Hg vapour to an anode A. Between the anode and the grid is a braking voltage of about 0.5 V. Electrons which have lost most of their kinetic energy in inelastic collisions in the gas-filled space

can no longer move against this braking potential and fall back to the grid. The anode current is then measured as a function of the grid voltage V_G at a constant braking potential V_B.

The result is shown in the lower part of Fig. 8.12. As soon as V_G is greater than V_B, the current increases with increasing voltage (space-charge conduction law). At a value of $V_G \cong 5$ V (in mercury vapour) the current I is strongly reduced; it then increases again up to $V_G \cong 10$ V, where the oscillation is repeated. The explanation of these results is found by making the following assumptions: when the electrons have

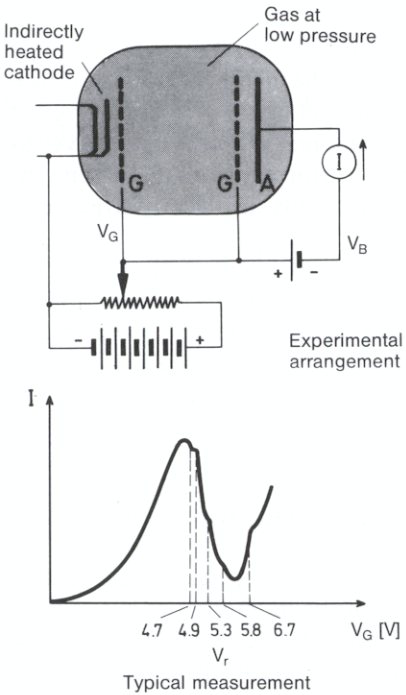

Fig. 8.13. Improved experimental setup for determining atomic excitation energies by electron collisions. The collisions take place in the field-free space between the two grids G. In this way, a high resolution is reached. In the lower part of the figure, an experimental result obtained with Hg vapour is shown in part

reached an energy of about 5 eV, they can give up their energy to a discrete level of the mercury atoms. They have then lost their energy and can no longer move against the braking potential. If their energy is 10 eV, this energy transfer can occur twice, etc. Indeed, one finds an intense line in emission and absorption at $E = 4.85$ eV in the optical spectrum of atomic mercury, corresponding to a wavelength of 2537 Å. This line was also observed by *Franck* and *Hertz* in the optical emission spectrum of Hg vapour after excitation by electron collisions. The excitation or resonance voltages are denoted in Figs. 8.12, 13 as V_r.

The resolving power for the energy loss of the electrons may be improved by using an indirectly heated cathode and a field-free collision region. In this way, one obtains a better uniformity of the energies of the electrons. With an improved experimental arrangement (Fig. 8.13), a number of structures can be seen in the current-voltage curve; these correspond to further excitations of the atoms. The step at 6.73 eV, for example, corresponds to a further intense line in the Hg spectrum; 6.73 eV $\triangleq$ 1850 Å.

Not all the maxima in the current-voltage curve can be correlated with observed spectral lines. To explain this fact, we have to assume that optically "forbidden" transi-

tions can, in some cases, be excited by collisions. We shall see later that there are selection rules for optical transitions between energy terms of atoms, according to which not all combinations of terms are possible – one says "allowed". The selection rules for collision excitation of atoms are clearly not identical with those for optical excitation (or de-excitation).

In this connection, the following experiment is interesting: Na vapour at low pressure can be excited to fluorescence by illumination with the yellow Na line (quantum energy 2.11 eV). The excitation occurs only when the light used for illumination has exactly the quantum energy 2.11 eV. Both smaller and larger quantum energies are ineffective in producing an excitation.

Excitation by means of collisions with electrons are in this respect quite different: in this type of excitation, the yellow line is emitted whenever the energy of the electrons is equal to or *larger than* 2.11 eV. This can be explained as follows: the kinetic energy of free electrons is not quantised. After excitation of a discrete atomic energy level by electron collision, the exciting electron can retain an arbitrary amount of energy, depending on its initial value. This remaining energy can, if it is sufficiently large, serve to excite still other atoms in the gas volume.

All in all, these electron collision experiments prove the existence of discrete excitation states in atoms and thus offer an excellent confirmation of the basic assumptions of the Bohr theory. In modern atomic and solid state physics, energy-loss spectra of electrons represent an important aid to the investigation of possible excitation stages of atoms and of the structure of the surfaces of solids.

8.9 Sommerfeld's Extension of the Bohr Model and the Experimental Justification of a Second Quantum Number

The finished picture of the Bohr model still contained some fuzzy details: exact spectral measurements at high resolution showed that the lines of the Balmer series in hydrogen are, in fact, *not* single lines. Each of them consists rather of several components; how many one can distinguish depends on the resolution of the spectrometer employed.

The H_α line of hydrogen with $\bar{\nu} = 15233\ \mathrm{cm}^{-1}$ consists, for example of a multiplet with a wavenumber splitting of $\Delta\bar{\nu} = 0.33\ \mathrm{cm}^{-1}$ between the strongest components (Fig. 8.14). In order to observe this structure, a spectral resolution of nearly $\bar{\nu}/\Delta\bar{\nu} = 100\,000$ is needed. In the spectrum of the one-electron ion He^+, these multiplet lines are more strongly separated, and the splitting is therefore easier to observe. We shall see in Chap. 12 that the splitting increases as the 4th power of the nuclear charge number Z.

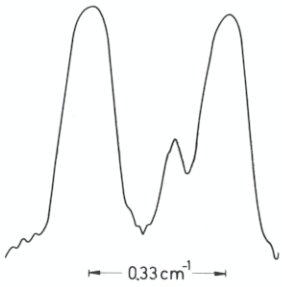

Fig. 8.14. H_α line of the Balmer series at a high spectral resolution. Three components can be distinguished. A still higher resolution is shown in Fig. 12.24. The resolution reached in this spectrum is limited by Doppler broadening

From observations of this type, *Sommerfeld* derived an extension of the Bohr model. It is well known from classical mechanics that, according to Kepler's Laws, not only circular orbits, but also elliptical orbits are possible, having the same energies.

From this, *Sommerfeld* drew the conclusion that the same is true in atoms also. In order to distinguish the elliptical orbits from the circular ones, a new, second quantum number is required. Since *Sommerfeld*'s chain of reasoning was on the one hand of great historical importance in introducing a second quantum number, but has, on the other hand, been made obsolete by the later quantum mechanical treatment, we will only give a brief summary here.

The principal quantum number n remains valid; it continues to determine the total energy of a term according to (8.20), i.e.

$$E_n = -\frac{RhcZ^2}{n^2}. \tag{8.34}$$

According to *Sommerfeld*, n also determines the major semiaxis of the ellipse. The minor semiaxis is determined by the second quantum number in such a fashion that the absolute value of the angular momentum remains a whole multiple k of $\hbar$, with $k \leqq n$. The length of the minor semiaxis, that is the eccentricity of the ellipse, has in this model no influence on the total energy. Each principal quantum number n corresponds to one major semiaxis a_n, but to various orbital shapes, characterised by the minor semiaxis $b_{n,k}$. We say that the energy term is n-fold degenerate, by which is meant that different orbits with two quantum numbers n and k belong to one and the same energy value.

We should mention at this point that in quantum theory, the Sommerfeld second quantum number k became the orbital angular momentum quantum number $l (l = k-1)$. The orbital angular momentum of the electron is given by (as we shall show in Chap. 10)

$$|\boldsymbol{l}| = \sqrt{l(l+1)}\,\hbar \quad \text{with} \quad l = 0, 1, 2, \ldots n-1\,. \tag{8.35}$$

In order to distinguish the orbital angular momentum itself, $\boldsymbol{l}$, from its quantum number l, we shall henceforth use the symbol $|\boldsymbol{l}|$ for the absolute value of the angular momentum vector $\boldsymbol{l}$.

For the various numerical values of the angular momentum quantum number, letter symbols s, p, d, f, g, h, etc. have become firmly established; these are listed in the following table:

Quantum number	$l = 0$	1	2	3	4	5
Angular momentum	$\lvert\boldsymbol{l}\rvert = 0$	$\sqrt{2}\,\hbar$	$\sqrt{6}\,\hbar$	$\sqrt{12}\,\hbar$	$\sqrt{20}\,\hbar$	$\sqrt{30}\,\hbar$
Name (Symbol)	s	p	d	f	g	h-electron or state.

What this means in terms of the spatial form of the electron orbitals will be explained later, together with the solution of the Schrödinger equation (Chap. 10).

8.10 Lifting of Orbital Degeneracy by the Relativistic Mass Change

We still have no explanation for the doublet or multiplet structure of the spectral lines mentioned at the beginning of the last section. However, we now know that each level is n-fold degenerate; by this we mean the fact that each energy level has various possibilities for the spatial distribution of the electrons occupying it. The number of levels with differing energies, and thus the number of observable spectral lines, however still remains the same.

The lifting of this degeneracy occurs, according to *Sommerfeld* (1916), through the effect of the relativistic mass change, $m = m(v)$, which we have neglected up to now. We can understand this qualitatively as follows: exactly as in planetary motion according to Kepler's Laws, the electrons are accelerated when they come near to the nucleus. This is a result of Kepler's Law of Areas, which requires that the moving electron sweep out equal areas between its orbit and the nucleus in equal times. In the neighbourhood of the nucleus, the electrons are thus faster and, from special relativity, more massive. This leads, in turn, to a decrease in energy: increased mass means, according to *Bohr*, a smaller radius, and this leads to a larger (negative) binding energy, i.e. to a decrease in total energy. The smaller the minor semiaxis of an ellipse, the more significant these relativistic corrections must become.

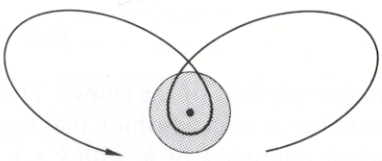

Fig. 8.15. Rotation of the perihelion point in the motion of an electron around the nucleus in a many-electron atom according to the Sommerfeld theory. The shaded region is the electronic shell of the atom. The outer electron follows a so-called "diving orbit" in its motion, i.e., it dives into the atomic shell. This model provides an intuitive explanation of the lifting of orbital degeneracy due to the relativistic mass effect (Sect. 8.10) and to the shielding of the nuclear charge (see Sect. 11.2)

We will not repeat *Sommerfeld*'s calculation here; we just give the result. The relativistic mass change leads to a rotation of the perihelion point of the orbits; in an intuitive picture, the electron then has a "rosette motion" about the nucleus (Fig. 8.15).

In *Sommerfeld*'s calculation, the "fine structure constant" plays a rôle:

$$\alpha = \frac{\text{Velocity of the electron in the 1st Bohr orbit}}{\text{Velocity of light}}$$

$$= \frac{e^2}{2\varepsilon_0 hc} = \frac{1}{137} \quad \text{(dimensionless)} .$$

For an electron orbit with the quantum numbers n and k, the result of *Sommerfeld*'s calculation of the relativistic mass effect is

$$E_{n,k} = -Rhc\frac{Z^2}{n^2}\left[1 + \frac{\alpha^2 Z^2}{n^2}\left(\frac{n}{k} - \frac{3}{4}\right) + \text{higher-order corrections}\right]. \qquad (8.36)$$

The relativistic energy change is thus of the order of $\alpha^2 \cong 10^{-5}$, i.e. small, but observable (see Fig. 8.14). Applying the models developed by *Sommerfeld*, the structures of the hydrogen atom mentioned thus far can be described both qualitatively and quantitatively. However, further experiments, which we shall describe in Chap. 12, pointed out the limits of these models. An adequate description of the relativistic motion of the electron is provided by the Dirac equation (cf. Sect. 14.6).

8.11 Limits of the Bohr-Sommerfeld Theory. The Correspondence Principle

The Bohr-Sommerfeld model is theoretically unsatisfying: on the one hand, classical mechanics is set aside, and only certain particular orbits are allowed; on the other hand, classical physics is used to calculate the orbits, see Sect. 8.3. It is as though, "On Mondays, Wednesdays and Fridays one uses the classical laws, on Tuesdays, Thursdays, and Saturdays the laws of quantum physics" (*Bragg*). Furthermore, the model predicts only the frequencies but not the intensities or the time dependence of emitted or absorbed light.

The gap which had opened between classical physics and the (early) quantum theory was bridged by *Bohr* with his *Correspondence Principle*.

According to this principle, for large quantum numbers, the classical and quantum theories approach one another; or, the behaviour of an atom approaches that expected from classical, macroscopic physics, the larger its energy relative to the energy change which occurs in the process considered, i.e. all the more, the higher the level and the smaller the level difference.

Starting from considerations such as the above, one arrives at the following general formulation of the Correspondence Principle:

Every non-classical theory must, in the limit of high energies and small energy changes, yield the results of classical theory.

The intensities, polarisations, and selection rules for spectral lines may be calculated from the laws of classical physics. The Correspondence Principle allows us, within limits, to translate these results, by using a prescription for quantisation, into the quantum theory.

In spite of a series of successes, the application of the Bohr-Sommerfeld theory led to fundamental difficulties. The results were wrong even for atoms with two electrons. The magnetic properties of atoms were not correctly described. The removal of these difficulties was accomplished with the development of modern quantum mechanics. In Chap. 10, we will treat the hydrogen atom problem exactly with the help of quantum theory; we shall find there that some of the results of the Bohr-Sommerfeld theory remain valid, while others must be modified.

8.12 Rydberg Atoms

Atoms in which an electron has been excited to an unusually high energy level illustrate well the logical continuity between the world of classical physics and quantum mechanics.

Such atoms, called Rydberg atoms, have extraordinary properties. They are gigantic: Rydberg atoms are known with diameters reaching 10^{-2} mm, corresponding to a 100000-fold increase over the diameters of atoms in the ground state. Furthermore, these excited states have *extremely long lifetimes.* While typical lifetimes of lower excited states of atoms are about 10^{-8} s, there are Rydberg atoms which have lifetimes of 1 s. The difference in energy between two neighboring states n and n' becomes very small when n is large. The long lifetimes of such states are in part a result of the fact that the probability of a spontaneous transition between two states n and n' is, according to Einstein (Sect. 5.2.3), proportional to ν^3. In addition, Rydberg atoms may be *strongly polarised* by relatively weak electric fields, or even completely ionised.

When the outer electron of an atom is excited into a very high energy level, it enters a spatially extended orbit – an orbital – which is far outside the orbitals of all the other electrons. The excited electron then "sees" an atomic core, consisting of the nucleus and all the inner electrons, which has a charge $+e$, just the same as the charge of the hydrogen nucleus. As long as the excited electron does not approach the core too closely, it behaves as though it belonged to a *hydrogen atom.* Rydberg atoms behave therefore in many respects like highly excited hydrogen atoms.

In interstellar space, there are atoms whose outer electrons are in states with principal quantum numbers n up to 350; this has been observed by radio astronomical methods. In the laboratory, Rydberg atoms with principal quantum numbers between 10 and 290 have been studied. A recent example of still larger values of n is shown in Fig. 8.18.

The orbital radius of an electron in an atom is proportional to n^2 (8.17). The spacing between neighbouring energy levels decreases as n^{-3}. It is because these higher powers of n have especially large effects for large n-values that Rydberg atoms have their unusual properties.

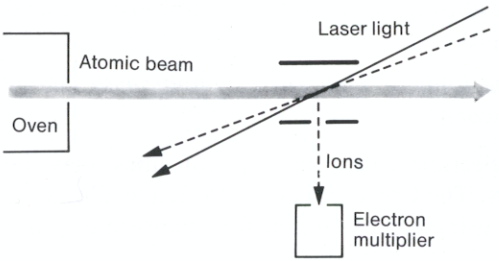

Fig. 8.16. Apparatus for the detection of Rydberg atoms. An atomic beam is crossed by several (here 2) laser beams. They cause the excitation of the atoms into Rydberg states when the sum of the quantum energies of the laser beams corresponds to the excitation energy of a Rydberg state. The Rydberg atoms are ionised in the electric field of a condenser, and the ions are then detected

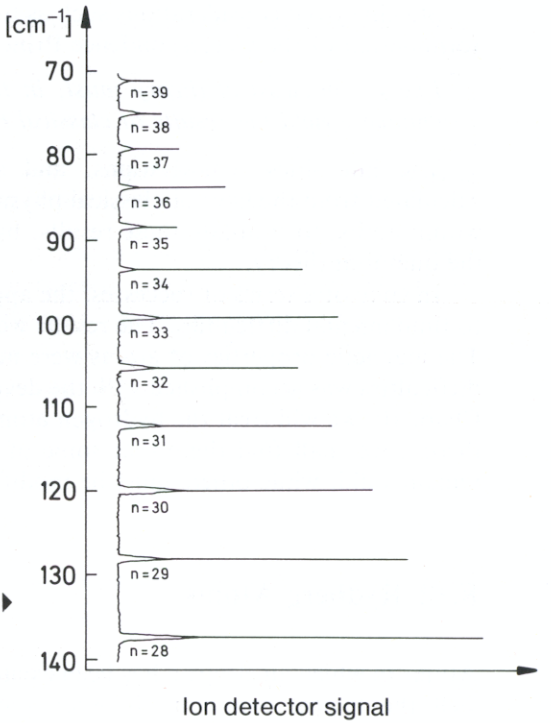

Fig. 8.17. An example of the detection of Rydberg states of the lithium atom with $n = 28$ to 39, measured with an apparatus like that shown in Fig. 8.16. The distance (in wave number units) to the series limit is plotted as the ordinate

Rydberg atoms are produced by exciting an atomic beam with laser light. To detect the highly excited atoms, an electric field is applied between the plates of a condenser through which the atomic beam passes. Through field ionisation, the atoms can be converted to ions with the aid of small electric fields of the order of a few hundred V cm^{-1}. The ions can be detected by means of their charge, for example with the aid of an electron multiplier or channeltron. An example of an experimental setup is shown in Fig. 8.16; Fig. 8.17 shows some experimental results. In Fig. 8.17, the result of exciting a beam of lithium atoms with three laser beams is shown. The first two excite the atoms into intermediate excited states (e.g. here $n = 3$, $l = 0$), while the third is continuously variable within a small energy range and adds the last necessary energy contribution to put the atoms into a Rydberg state. By continuously changing the frequency of this last laser, the experimenter can excite a series of Rydberg states of the atoms one after another – in the figure, the states with $n = 28$ to 39. Thus, a particular Rydberg state can be chosen and selectively excited in order to investigate its physical properties.

When a Rydberg atom reduces its principal quantum number by 1 in emitting a light quantum, the light is in the far infrared or microwave region of the electromagnetic spectrum. With this radiation, isolated Rydberg atoms were first discovered in 1965 in interstellar space. The density of atoms is so low there that collisions are extremely rare.

It has been possible to investigate Rydberg atoms in the laboratory since narrow-band, tunable lasers have been available (especially dye lasers, see Chap. 21). Since then, the energy levels, lifetimes, spatial extension of the wavefunctions, and the influence of electric and magnetic fields have been studied for quantum numbers which were previously only theoretical. The predictions of theory have been fully confirmed. Table 8.8 contains an overview of the properties of Rydberg atoms.

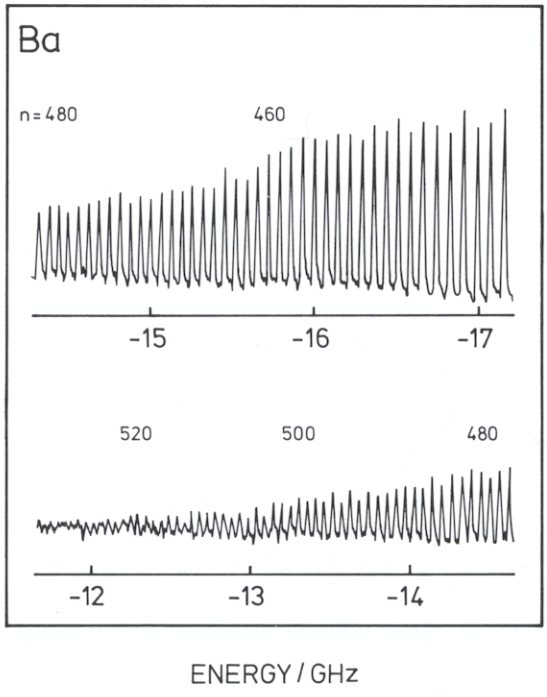

Fig. 8.18. Rydberg excitation states of barium atoms with the principal quantum number n, observed using Doppler-free spectroscopy. The abcissa gives the distance from the series limit in units of GHz. From J. Neukammer et al.: Phys. Rev. Lett. **59**, 2947 (1987)

Table 8.8. Some properties of Rydberg atoms, valid for unperturbed electronic states

Property	General	Rydberg atoms, $n = 30$
Size	$d = a_0 n^2$	10^3 Å
Binding energy	$-E_n = R_\infty / n^2$	10^{-2} eV
Transition energy $\Delta n = 1$	$\Delta E = 2R/n^3$	10^{-3} eV $\triangleq 10$ cm^{-1}
Lifetime	$\tau \propto n^3$	$30 \cdot 10^{-6}$ s

8.13 Positronium, Muonium, and Antihydrogen

It is possible to make artificial atoms in which one or both of the atomic components of hydrogen, the proton and the electron, are replaced by their corresponding antiparticles. The antiparticle of the proton is the antiproton, $\bar{p}$; that of the electron is the positron, e^+. As far as is currently understood, particles are distinguished from their antiparticles only through the opposite sign of their electric charges and magnetic moments, cf. Sect. 14.6. Therefore, all the conclusions of the Bohr model concerning atomic radii, energy levels, and transition frequencies derived in Sects. 8.4 and 8.5 should also apply to atoms containing antiparticles. Here, we shall treat briefly the "exotic" atoms positronium, muonium, and antihydrogen.

Positronium, an "atom" consisting of an electron, e^-, and a positron, e^+, was discovered in 1949 by *M. Deutsch*. It is formed when positrons and electrons enter a

Table 8.9. The reduced mass m_r in units of the electron mass, the binding energy E_B, the energy spacing between the $n = 1$ and $n = 2$ levels, and the first Bohr radius a_0 for positronium and muonium in comparison to the H atom

		$\frac{m_r}{m_0}$	E_B	$E_2 - E_1$	a_0
Hydrogen	$p^+ e^-$	≈ 1	13.6 eV	10.2 eV	0.53 Å
Positronium	$e^+ e^-$	0.5	6.8 eV	5.1 eV	1.06 Å
Muonium	$\mu^+ e^-$	≈ 1	13.6 eV	10.2 eV	0.53 Å

(short-lived) bound state ($e^+ e^-$), before they annihilate each other with the emission of two γ-quanta. If the particles have no kinetic energy before their annihilation, each of the γ-quanta has an energy equal to $m_0 c^2 = 511$ keV, where m_0 is the mass of the electron. The lifetime of socalled parapositronium, with overall spin $S = 0$ (see Sect. 17.3), is $1.25 \cdot 10^{-10}$ s. Orthopositronium, with $S = 1$, is produced with a smaller probability and has a longer lifetime of $1.4 \cdot 10^{-7}$ s. It decays into 3 or more γ-quanta.

Positrons can be obtained from the radioactive decay of nuclei, e.g. of ^{22}Na, and are thus relatively readily available. Positronium atoms are formed when positrons pass through a gas or impinge on solid surfaces, where the positron can capture an electron. During the brief lifetime of the atoms, their binding energies and excitation energies can be measured and the results of the Bohr model thus confirmed.

According to (8.20) and (8.22), the energies of the levels should be proportional to the reduced mass, and therefore half as large as in the hydrogen atom. The orbital radii and the wavelengths of the emitted radiation should be twice as large as in hydrogen. Both effects are observed as predicted; cf. Table 8.9.

In condensed-matter physics and in modern medicine, positronium atoms are used as probes for structures and dysfunctions, because the emission of their annihilation radiation, and thus their lifetimes, is dependent on their material surroundings. In medicine, positron emission tomography is used for example to form an image of diseased tissue in the brain.

Muonium, ($\mu^+ e^-$), is so to speak the lightest muonic atom (cf. Sect. 8.7). It is formed in a similar way to positronium, when positive muons, μ^+, enter into a bound state with electrons on passing through a gas or on a solid surface. Like negative muons, μ^+ particles are unstable (see Sect. 8.7), and the lifetime of muonium is correspondingly only $2.2 \cdot 10^{-6}$ s. According to (8.20) and (8.22), its binding energy is 13.5 eV, only slightly different from that of hydrogen, due to the nearly equal reduced masses. The orbital radii are obtained from (8.17), and the lowest optical excitation from the state with $n = 1$ ($1S$ state) to the state with $n = 2$ ($2S$) is found from (8.21) to be 10.15 eV; cf. also Table 8.7. These atoms have been studied extensively by spectroscopic methods, but we will not discuss the results further here. They are particularly relevant to the refinements of the Bohr model by Dirac's relativistic quantum mechanics, which we will treat in Chap. 12.

Particularly interesting is the *antihydrogen atom*, ($\bar{p} e^+$), which consists of a positron bound to a negatively-charged antiproton. According to the postulates of quantum mechanics, antimatter should behave just like ordinary matter. An experimental test has yet to be performed, since antimatter was not available until very recently. In 1995, the successful preparation of antihydrogen was reported for the first time. It was carried out as follows:

Antiprotons can be produced in accelerators having particle beams of sufficiently high energy, for example at CERN in Geneva. When they pass through the Coulomb field of an atomic nucleus (xenon gas was used), a portion of the kinetic energy of the antiprotons is converted into e^+/e^- pairs. With a small probability, the slowed antiproton $\bar{p}$ can capture a positron e^+, giving rise to an atom of antihydrogen, $(\bar{p}\,e^+)$. It is electrically neutral and therefore leaves the accelerator ring on a tangential orbit.

Thus far, these antihydrogen atoms have been detected only via their decays: the e^+ is stripped off the atom when it passes through a Si semiconductor particle detector. This positron annihilates with a negative electron, and the resulting annihilation radiation is detected and measured by a NaI scintillation counter. The remaining $\bar{p}$ is analysed with respect to its mass, charge, and velocity by additional detectors. In the first report (by the group of *W. Oelert*, in Phys. Lett. **B** (1996)), the detection of 8 antihydrogen atoms is described; they were produced by a beam of 10^{10} antiprotons during a beam time of 15 hours. Their lifetime was about 40 ns.

One goal of such efforts is the spectroscopic investigation of the antihydrogen atoms, as a test of the symmetry of the interactions between matter and antimatter. For this purpose, e.g. for the observation of the Balmer series of antihydrogen, the very few atoms as yet produced, which in addition have high kinetic energies and short lifetimes, are naturally not sufficient.

Another experiment designed to produce antihydrogen is planned to yield the atoms in a state of rest, without kinetic energy, by using a combination ion trap for positive heavy and negative light particles (cf. Sect. 2.4.6) and trapping antiprotons and positrons in it at the same time. The group of *Th. Hänsch* has already reported the simultaneous trapping of positive and negative particles in such a combined trap (Phys. Rev. Lett. **75**, 3257 (1995)). The binding of trapped particles to antihydrogen has however not yet been observed.

Problems

8.1 Calculate the recoil energy and velocity of a hydrogen atom in a transition from the state $n = 4$ to the state $n = 1$, in which a photon is emitted.

8.2 Five of the Balmer series lines of hydrogen have the wavelengths 3669.42 Å, 3770.06 Å, 3835.40 Å, 3970.07 Å and 4340.47 Å. Plot $\bar{\nu}$ as a function of n for the Balmer series. From this, determine the value of n for the upper level of each of the five wavelengths above.

8.3 The absorption spectrum of hydrogen can be obtained by allowing white light to pass through hydrogen gas which is in the ground state and contains atomic hydrogen (not just H_2). Which photon energies are observed in the hydrogen absorption spectrum? Give the wavelengths of these "Fraunhofer lines".

8.4 a) The emission spectrum of the hydrogen atom is taken with a diffraction grating (line spacing $d = 2$ μm). A line of the Balmer series is observed in the second order at an angle $\theta = 29°5'$. What is the quantum number of the excited state from which the transition starts?

b) What is the minimum number of lines necessary in a diffraction grating if the first 30 spectral lines of the Balmer series of the hydrogen atom are to be resolved in the first-order diffraction spectrum?

Hint: In this case, the number of lines corresponds to the required resolution $\lambda/\Delta\lambda$.

8.5 Is it true that in a circular Bohr orbit, the potential energy is equal to the kinetic energy? If not, where does the energy difference go which arises if we assume that the electron and the nucleus are initially infinitely far apart and at rest? How large is E_{pot} compared to E_{kin} for the various Bohr orbits?

8.6 The attractive force between a neutron (mass M) and an electron (mass m) is given by $F = GMm/r^2$. Let us now consider the smallest orbit which the electron can have around the neutron, according to Bohr's theory.

a) Write a formula for the centrifugal force which contains m, r and v; r is the radius of the Bohr orbit, and v is the velocity of the electron in this orbit.
b) Express the kinetic energy in terms of G, M, m and r.
c) Express the potential energy in terms of G, M, m and r.
d) Express the total energy in terms of G, M, m and r.
e) Set up an equation which corresponds to the Bohr postulate for the quantisation of the orbits.
f) How large is the radius r of the orbit with $n = 1$? Express r in terms of $\hbar$, G, M and m; give the numerical value of r.

8.7 For the Bohr model of the atom, calculate the electric current and the magnetic dipole moment of the electron in the first three orbits ($n = 1, 2, 3$).

Hint: Use (12.1 – 7) to calculate the magnetic dipole moment.

8.8 "Positronium" is a bound electron-positron pair. The positron is the anti-particle corresponding to the electron. It has a charge $+e$ and the same rest mass as the electron. On the assumption that e^- and e^+ – in analogy to the H atom – circle the common centre of gravity, calculate the rotational frequency ω, the radius r and the binding energy of the system in the ground state.

8.9 A muonic atom consists of an atomic nucleus with nuclear charge Z and a captured muon, which is in the ground state. The muon is a particle with a mass 207 times that of the electron; its charge is the same as that of the electron.

a) What is the binding energy of a muon which has been captured by a proton?
b) What is the radius of the corresponding Bohr orbit with $n = 1$?
c) Give the energy of the photon which is emitted when the muon goes from the state $n = 2$ to the ground state.

8.10 Estimate the number of revolutions N an electron makes around the nucleus in an excited hydrogen atom during the average lifetime of the excited state – 10^{-8} s – if a) it is in the state with $n = 2$, and b) in the state with $n = 15$, before it returns to the $n = 1$ state. c) Compare these numbers with the number of revolutions the earth has made around the sun in the 4.5×10^9 years of its existence.

8.11 In addition to the isotope ^{4}He, natural helium contains a small amount of the isotope ^{3}He. Calculate the differences in the wavenumbers and energies of the first and third lines of the Pickering series which result from these mass differences. The relative isotopic masses are:

^{3}He: 3.01603 u and ^{4}He: 4.00260 u .

8.12 Which lines of the hydrogen spectrum lie in the visible region of the spectrum (between 4000 Å and 7000 Å)? Which helium lines fall in the same region? How could one tell whether a helium sample has been contaminated with hydrogen?

8.13 Estimate the relative relativistic correction $\Delta E_{n,k}/E_n$ for the $n = 2$ levels in the hydrogen atom.

Hint: Compare (8.29).

8.14 To excite the hydrogen atom into its Rydberg states, one uses the additive absorption of the light from two lasers. Let the first of these have a fixed emission wavelength λ, which corresponds to 11.5 eV. What wavelengths must the second laser have in order to pump atoms into the state with $n = 20$, 30, 40 or 50? How large are the radii and binding energies for these states? What is the maximum possible linewidth for both lasers if only a single n state is to be populated?

8.15 a) Calculate the frequency of the orbital motion of an electron in a hydrogen atom for a level with the quantum number n.

b) Calculate the frequency of the radiation emitted in the transition from the state n to the state $n-1$.

c) Show that the results of a) and b) agree if n is very large.

8.16 Estimate the magnitude of the correction terms which must be applied to the energies of the stationary states of the lightest atoms, i.e. ^1H, ^2H, ^3H, He^+ and Li^{2+}, to account for the motion of the nucleus.

8.17 If one did the Franck-Hertz experiment on atomic hydrogen vapour, which lines in the hydrogen spectrum would one see if the maximum energy of the electrons were 12.5 eV?

8.18 Four lines in the Balmer series of He^+ have the wavelengths 164.05 nm, 121.52 nm, 108.45 nm, and 102.53 nm. Plot the wavenumbers $\bar{\nu}$ as a function of n. Is there a more reasonable way to plot these data? Find the value of n in the upper level for each of the wavelengths given.

Hint: What is the meaning of the Balmer series? He^+ is analogous to H.

8.19 A Wannier exciton is a bound state between an electron and a hole in a solid. Apply the Bohr model to such an electron-hole pair, taking the effective masses and the dielectric constant of the semiconductor (surrounding medium) into account.

a) What are the energies of the excited states with $2 \leq n \leq 5$?

b) What does the absorption spectrum of such an exciton book like?

Hint: A hole is a missing electron, which ideally has the same properties as an electron except for its positive charge. As an example, consider Cu_2O, with $\varepsilon_r \approx 10$, reduced mass $\mu \approx 0.7\, m_0$. Literature: C. Kittel: *Introduction to Solid State Physics.*